Nine Outstanding Questions of Solar Wind Physics

Nicholeen M. Viall[1], and Joseph E. Borovsky[2]

[1] NASA Goddard Space Flight Center, Greenbelt, Maryland 20771 USA.

[2]Center for Space Plasma Physics, Space Science Institute, Boulder, Colorado 80301 USA.

Corresponding author: Nicholeen Viall (Nicholeen.M.Viall@nasa.gov)

Key Points:

1. Nine outstanding questions of solar wind physics are synthesized from inputs from the heliospheric research community.

2. New ways of viewing these questions are put forth and suggestions for future progress are offered.

3. Calls are made for improved measurements, simulations, and plasma-physics theory.

Plain language summary

The Sun's atmosphere, called the solar corona, is a very hot plasma (ions and electrons) that reaches temperatures of 1,000,000 K or more. The coronal plasma continually expands away from the Sun, carrying solar magnetic field with it. This is the solar wind. It reaches speeds of hundreds of kilometers per second and fills the solar system. The space carved out by the solar wind flow defines the Heliosphere. The formation of the solar wind and its evolution as it flows away from the Sun is fundamental to how the Sun and stars get rid of stressed magnetic fields, and involves physical processes that operate throughout the universe. Additionally, the solar wind constantly bombards Earth's magnetic field and plasma environment, driving dynamics called space weather. The solar wind is the medium through which larger space weather events from solar storms propagate. Understanding the solar wind is therefore key for understanding the space environment around Earth. In this paper we synthesize input from the Heliophysics community on the outstanding questions of solar wind physics. We describe the current state of research, an updated framework for understanding solar wind formation, and future needs and

opportunities for progress, including what is likely to be accomplished in near future with data from Parker Solar Probe, from Solar Orbiter, from the Daniel K. Inouye Solar Telescope (DKIST), and from Polarimeter to Unify the Corona and Heliosphere (PUNCH).

Abstract: In situ measurements of the solar wind have been available for almost 60 years, and in that time plasma-physics simulation capabilities have commenced, and ground-based solar observations have expanded into space-based solar observations. These observations and simulations have yielded an increasingly improved knowledge of fundamental physics and have delivered a remarkable understanding of the solar wind and its complexity. Yet there are longstanding major unsolved questions. Synthesizing inputs from the solar wind research community, nine outstanding questions of solar-wind physics are developed and discussed in this commentary. These involve questions about the formation of the solar wind, about the inherent properties of the solar wind (and what the properties say about its formation), and about the evolution of the solar wind. The questions focus on (1) origin locations on the Sun, (2) plasma release, (3) acceleration, (4) heavy-ion abundances and charge states, (5) magnetic structure, (6) Alfven waves, (7) turbulence, (8) distribution-function evolution, and (9) energetic-particle transport. On these nine questions we offer suggestions for future progress, forward looking on what is likely to be accomplished in near future with data from Parker Solar Probe, from Solar Orbiter, from the Daniel K. Inouye Solar Telescope (DKIST), and from Polarimeter to Unify the Corona and Heliosphere (PUNCH). Calls are made for improved measurements, for higher-resolution simulations, and for advances in plasma-physics theory.

1. Introduction: What have been the obstacles to progress in solar wind physics?

The solar wind is the hot, supersonic flow of plasma and magnetic field from the Sun that defines the heliosphere. It has been studied with in situ measurements since the 1960s (Ness, 1996; Neugebauer, 1997; Obridko and Vaisberg, 2017). Excellent reviews of the rapid progress of solar wind physics can be found (e.g. Schwenn and Marsch, 1991a, b; von Steiger, 2008; Schrijver and Siscoe, 2009; Paz Miralles and Sanchez, 2011; Cranmer et al. 2017). Decade after decade,

advancements in modeling, instrumentation, and remote observations have resulted in major progress toward understanding the solar wind and its fundamental physics.

Despite these advancements, there are still major outstanding questions regarding the solar wind formation and its evolution. The overarching challenge that has hindered progress is the need for observations and modeling that encompass scale sizes small enough to resolve kinetic physics up through the global scales of the system. In the solar wind, these are in situ measurement timescales of milliseconds (e.g. to capture the spatial scales of electron physics) up through global time scales of at least a solar rotation, a span of eight orders of magnitude. This is a major challenge for models and observations. As a result, observations and models must focus on restricted regions of parameter space. Further, modeling must reduce the complexity of the phenomena it mimics: e.g. restricting the spatial scales and timescales, approximating the physical interactions, and reducing the dimensionality.

Observationally, the solar wind is sparsely sampled, making it even more difficult to link relevant time and spatial scales. The majority of observations consist of single point, in situ measurements made near 1 AU. Since the launch Wind in 1994, followed by Solar and Heliospheric Observatory (SOHO) in 1995, Advanced Composition Explorer (ACE) in 1997, and Deep Space Climate Observatory (DSCOVR) in 2015, there have been continuous plasma and field measurements at L1 to monitor the Earth-impacting solar wind (King and Papitashvili, 2005). In 2006, Solar Terrestrial Relations Observatory (STEREO) commenced two additional sets of in situ measurements at ~ 1 AU. The two STEREO spacecraft are on slightly different orbits than Earth so that they separate in longitude from each other and Earth with time. With the L1 monitors, they provide observations at three different longitudes at approximately the same times and latitudes. Inside of 1 AU, the two Helios spacecraft (Helios A was launched in 1974 and deactivated in 1985; Helios B was launched in 1976 and deactivated in 1979) provided sets of in situ measurements between 0.3 and 1 AU. Ulysses, launched in 1990 and ceased operation in 2009, provided the only out-of-ecliptic, latitude-dependent dataset. The Voyager 1 and 2 spacecraft, both launched in 1977, provide virtually the only solar wind measurements beyond 5 AU. A few planetary missions during their cruise provide measurements at these and other locations (e.g. Cassini), but these are for brief periods of time. Multi-point in situ measurements are needed to disambiguate spatial advection from time dynamics, as well for understanding how large and small

scales feedback on each other. Including all of the missions described above, there are typically only somewhere between five to ten spacecraft measuring the solar wind in situ at a given time. This comes nowhere close to covering the ~8 orders of magnitude of scale size necessary for understanding the Sun-heliosphere as a system, though opportunities to fill in some of this coverage with white light imaging of electron density (discussed below) are now coming online.

Another obstacle to solar wind physics is the artificial boundary between solar atmospheric physics and solar wind physics forced by different observational techniques, rather than by physics. Telescope-based solar physics is a much older field, with remote observations of the Sun going back hundreds of years (von del Luhe, 2009). It has historically been tied to the field of astrophysics, especially in the comparison of the Sun to other stars. Solar wind physics on the other hand is relatively young (decades), and its in-situ-based research community has often been more closely tied to geophysics, especially on the solar wind interaction with the Earth. The plasma-physics regimes of the Sun and solar atmosphere are very different from that of the solar wind (collisional versus collisionless; sub- versus super-Alfvénic and super-sonic; Reynolds numbers; plasma β, …), so modeling approaches, observing techniques, and physical intuition are not easily transferred from one regime to the other. The transition between these physical regimes rarely correspond to the boundaries between observational regimes, driven by the available observational techniques.

The advent of white light heliospheric imagers has bridged the artificial boundary between solar atmospheric and solar wind physics. Solar Mass Ejection Imager (SMEI) was groundbreaking (Jackson et al., 2004), and the Sun Earth Connection Coronal and Heliospheric Investigation (SECCHI) suite onboard STEREO (Howard et al., 2008) has made a significant leap forward in this technology. STEREO images from the corona through to 1 AU in white light with the combination of two coronagraphs and two heliospheric imagers on each spacecraft. The recently selected Polarimeter to Unify the Corona and Heliosphere (PUNCH) mission will produce high resolution, high sensitivity, global images of the corona through the solar wind. Solar Orbiter (Müller et al. 2013), currently scheduled to launch in February 2020, will carry a white light heliospheric imager, SoloHI (Solar Orbiter Heliospheric Imager) [Howard et al. 2019], enabling the imaging of the corona-to-solar wind connection from a higher inclination angle than ever before.

The field of heliophysics is progressing in a fashion such that the previously distinct regimes of solar physics and solar wind physics are finally connecting in quantitative ways. Both modeling and observational capabilities have reached the level of detail where studying the complex nature of the 3D, time dynamic Sun and its multitude of consequences in the heliosphere (in this case, the solar wind) is possible. Solar Orbiter has a suite of in situ instruments, including measurements of elemental composition and charge states of ions, as well as remote imaging in different wavelengths to link the solar atmosphere with the solar wind. After decades of planning (Feldman et al., 1990; Randolph, 1996), the launch of the Parker Solar Probe (Fox et al, 2016) in 2018 (previously planned as Starprobe, Solar Probe, and Solar Probe Plus), makes the connection of solar wind physics to solar physics now highly opportune. The first results from Parker Solar Probe have already provided important new constraints on solar wind physics. Bale et al. (2019) show evidence for plasma instabilities, as well as rapid reversals in the magnetic field lasting minutes called 'switchbacks' at larger amplitudes and at a higher occurrence rate than ever observed before. Kasper et al. (2019) use the strahl and velocity to show that these switchbacks take the form of S-shaped bends in the magnetic field, and also show the solar wind has a larger azimuthal velocity, (corotational with the solar corona) than theories predict. Howard et al. (2019) show evidence for the predicted dust free zone around the Sun. Additionally, they resolve small flux ropes, and small-scale density structures and fluctuations within streamers. Lastly, McComas et al (2019) highlights the importance of the magnetic field structure in the solar wind for energetic particle transport.

2. Nine Outstanding Questions of Solar Wind Physics

Table 1 lists the nine outstanding questions of solar wind physics that are discussed in this paper. The discussion of the nine questions is not ordered by importance, but rather into three groups according to how they arise in thinking about how the solar wind is formed (theme 1), how to interpret observations of solar wind (theme 2), and physical mechanisms that operate on solar wind formation and evolution through the heliosphere (theme 3). Note that the related topics of coronal mass ejections (CME) Kilpua et al. [2019] and magnetic reconnection [Hesse and Cassak 2019] are covered in other Grand Challenge papers.

147 Table 1 Nine outstanding questions of solar wind physics.

The formation of the solar wind
(1): From where on the Sun does the solar wind originate?
(2): How is the solar wind released?
(3): How is the solar wind accelerated?
Interpreting observations of solar wind parcels
(4): What determines the heavy-ion elemental abundances, the ionic charge states, and the alpha/proton density ratios in the solar wind? (And what do they tell us about the Sun?)
(5): What is the origin and evolution of the mesoscale plasma and magnetic-field structure of the solar wind?
Physical mechanisms operating on solar wind formation and evolution
(6): What is the Origin of the Alfvénic Fluctuations in the Solar Wind?
(7): How is solar-wind turbulence driven, what are its dynamics, and how is it dissipated?
(8): How do the kinetic distribution functions of the solar wind evolve?
(9): What are the roles of solar wind structure and turbulence on the transport of energetic particles in the heliosphere?

148

149

150 ***Theme 1, The formation of the solar wind***

151 The first overarching theme we discuss is the formation of the solar wind. It has long been known
152 that the magnetic field lines that thread the solar corona are rooted in the solar convection zone
153 where they are constantly stirred and energized, and it is this energy that is supplied by this
154 convection (plus the energy contained in emerging magnetic flux) that heats the solar atmosphere
155 and accelerates the wind. Understanding the detailed mechanisms for the conversion, transport,
156 and deposition of energy that heats coronal plasma, and that accelerates the solar wind is a major
157 outstanding question in Heliophysics.

158

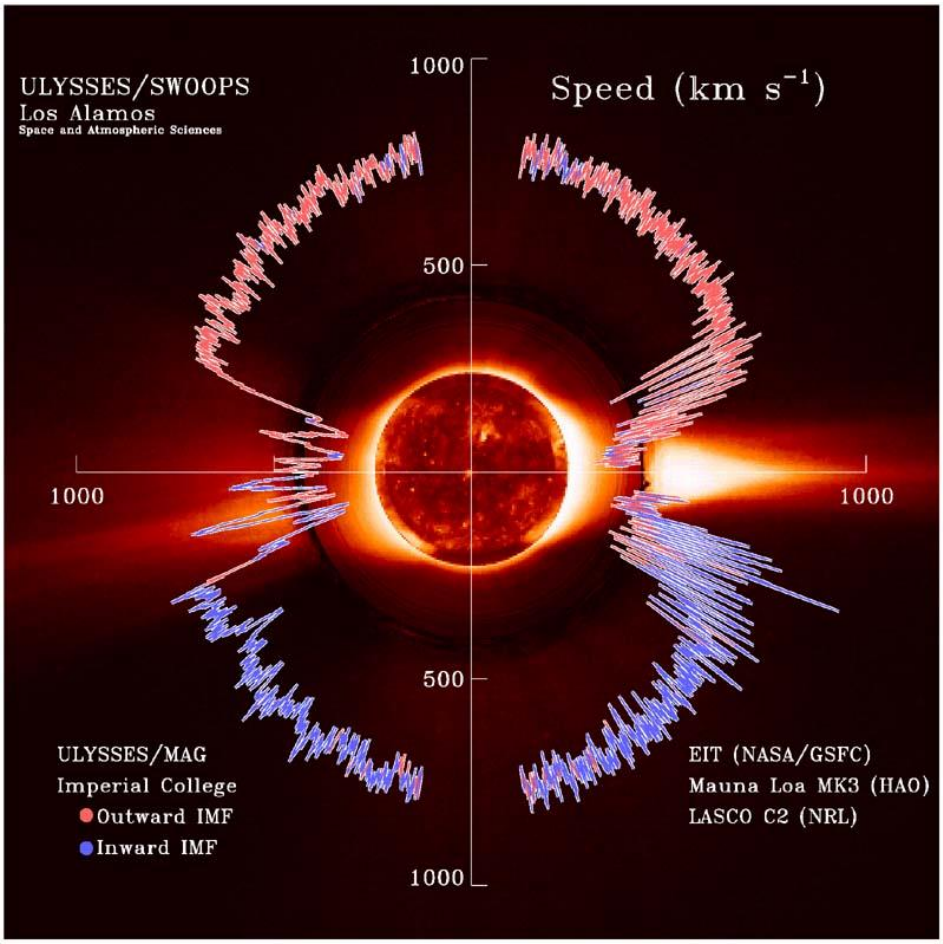

Figure 1, Solar wind speed and magnetic polarity measured by Ulysses, as a function of heliolatitude, overlaid with images from EIT, the HAO Mauna Loa coronagraph, and LASCO C2 coronagraph. Adapted from McComas et al. 1998.

Historically, the formation of the solar wind has been addressed using the well-known paradigm of two types of wind: a fast and a slow. The fast/slow paradigm has had a long history because it explains many of the global, average properties of the solar wind. Observations show that the slow solar wind is slower, denser, has higher charge states, lower alpha/proton abundance ratios, lower proton specific entropy, high variability in these properties, a lack of homogeneity, and lower Alfvénicity than the fast solar wind does. The slow wind also has higher abundances of elements with low first ionization potentials (FIP), similar to the abundances measured in the solar corona, while the fast wind has FIP abundances close to photospheric values. The Ulysses speed-versus-latitude plot (Figure 1) also illustrates the global fast/slow nature of the solar wind. This Ulysses plot demonstrates that the fast solar wind at high latitudes originates from areas of the solar corona called coronal holes that are cooler, and less dense, and so they produce less Extreme

Ultraviolet (EUV) emission than the rest of the corona. Note that the Ulysses data of Figure 1 were taken over five years (1992-1997), while the overlaid composite image of the solar atmosphere is from 17 August 1996. The composite image therefore does not capture any of the evolution of structure in the solar corona that occurred during the five years over which the Ulysses in situ measurements were taken. In the ecliptic, by association, fast, non-CME wind comes from the equatorial extensions of coronal holes (Krieger et al., 1973; Bame et al., 1976; Arge et al., 2004), and times when the magnetic dipole of the Sun (and therefore polar coronal holes) is tilted relative to the ecliptic. Also by association, slow wind is correlated with coronal streamers, which are observed at the same latitudes as the slow solar wind in Ulysses and ecliptic solar wind measurements. Coronal streamers are hotter, denser, and brighter than other regions of the solar corona.

The theoretical paradigm to explain these global fast and slow wind associations with coronal structures are divided into two general categories: waves/turbulence, or magnetic reconnection/loop opening (see review by Cranmer 2009). The two types of theories differ in the energization mechanism as well as the release mechanisms. In MHD wave/turbulence models, the release of solar wind plasma from the solar corona into the heliosphere occurs exclusively on open field lines. The energization that heats the corona and accelerates the wind is MHD waves and turbulence; the degree to which the open magnetic field expands with radius determines the nature of the energy deposition, resulting in slow and dense wind or fast and tenuous wind (Wang & Sheeley (1990) and Cranmer et al. (2007)). Heat conduction along the magnetic field is a crucial piece of the connection. In contrast, in the original theory of interchange reconnection to form the solar wind (Fisk 2003, Fisk et al., 1999; Tu et al., 2005) the release mechanism of the solar wind plasma from the corona is magnetic reconnection, and takes the form of 'interchange reconnection' wherein a closed magnetic field line reconnects with an open one (Crooker et al. 2002). The reconnection energizes the plasma, and smaller loops of closed magnetic field begin with cooler plasma that produce faster, tenuous wind, while larger, hotter loops produce, denser, slower wind.

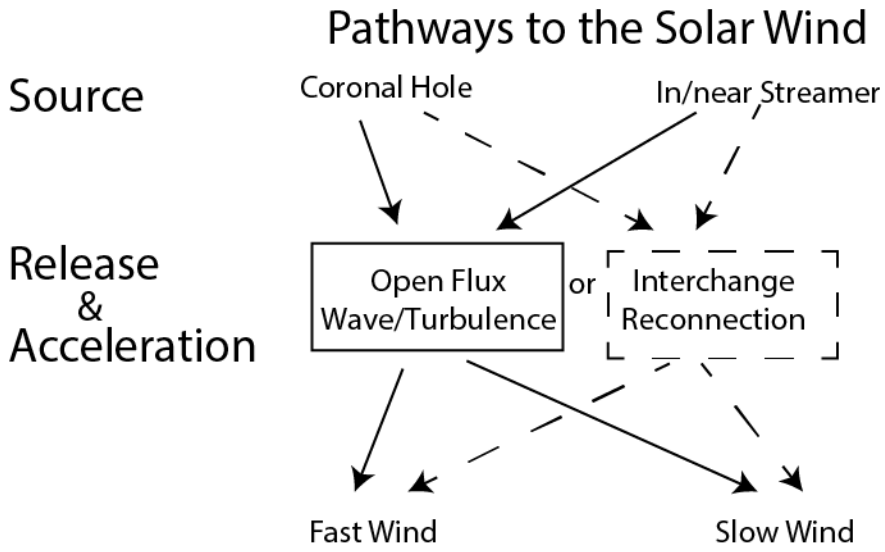

Figure 2 Historical paradigm to explain the pathway to the solar wind. There are only two sources: coronal holes and in/near streamers. The release mechanism and acceleration mechanism (dashed lines indicate interchange reconnection, solid indicates wave/turbulence on open fields) are linked, and the result is the fast and slow wind.

We illustrate this historical paradigm in Figure 2. The top indicates the two sources: coronal holes and inside or near streamers. The release and acceleration mechanisms are linked together, with the interchange reconnection (IR) paths in dashed lines, and wave/turbulence paths in solid. In the historical paradigm the outstanding question was: is it waves/turbulence on open flux, or is it reconnection of open flux with closed flux? The bottom of Figure 2 indicates the two options for types of wind in this paradigm: a fast wind or a slow wind.

We argue for a new framework for understanding solar wind formation. First, both reconnection and wave/turbulence theories can explain the long-term average fast/slow wind properties, which is one indication that it is time to refine the framework in a way that distinguishes between theories. Furthermore, there is a growing understanding that it is not accurate to treat different theories as mutually exclusive; rather, the relevant question is how much each theory plays a role in the solar wind formation. Some of these long-term relationships can be expressed as a scaling law, indicating that electromagnetic energy per particle added to the plasma is roughly fixed (Schwadron & McComas 2003). Since these energy balance requirements are satisfied on average and by many theories, locations and times where these long-term relationships are not satisfied are likely to provide new insights into the mechanisms at work. Indeed, there are

observations that show solar wind parcels that do not fit neatly into the historical paradigm. For example, there are wind parcels that are accelerated to slow speeds, but have composition and Alfvénicity of faster wind (Roberts et al. 1987; Stakhiv et al., 2015; D'Amics et al., 2019). Also not fitting the historical paradigm, observed solar wind charge states and speed distributions are not bimodal, but actually suggest a continuum of states (Zurbuchen et al. 1999).

Three examples of solar wind that do not fit neatly into the historical paradigm also illustrate a new way to understand the plasma pathway to the solar wind, which is to consider the time history of the plasma parcel. The first example is plasma blobs emitted from the tips of helmet streamers (located at the heliospheric current sheet, HCS). They are now known to be the result of reconnection at the HCS (Rappazzo et al. 2005; Sanchez-Diaz et al. 2017a, b; Kepko et al. 2016). In contrast to the interchange reconnection solar wind formation theory, as well as to coronal mass ejections, the reconnection that creates streamer plasma blobs is not observed to impart much acceleration or heating energy. Rather, the blobs appear to be carried along with the surrounding solar wind plasma as 'leaves in a stream', continuously accelerating for many solar radii after the reconnection occurs (Sheeley et al. 2009). This implies that even though magnetic reconnection is important for the release of the solar wind, a different physical mechanism than reconnection is responsible for the acceleration.

The second example is outflows (blueshifts) from the so-called 'fan loops' that are observed on the periphery of active regions in Hinode/EIS. The field lines associated with the fan loops and magnetic field of active regions are often open to the heliosphere, so the blue shifts have been interpreted as the nascent solar wind flow. However, many of these fan loops close at other locations on the Sun (Schrijver & DeRosa 2003), and the blue shifted outflows, as well as the temperatures of the fan loops, are independent of whether or not the field lines are open to Heliosphere (van Driel-Gesztelyi et al. 2012). Therefore, the coronal heating (i.e. the energization mechanism low in the corona) is independent of whether or not the plasma is released into the solar wind, and must be a separate physical step from acceleration.

The third example is the discovery of the type II spicule phenomena low in the solar atmosphere; it has been postulated that they could be formed as the result of reconnection (Samanta et al. 2019) and may contribute plasma to the corona and solar wind (De Pontieu et al., 2011). However, type II spicules are observed throughout the Sun, independent of their connection to the

heliosphere, as was the case in the fan loop example. In the case of type II spicules, if the plasma is on a field line connected the heliosphere, the plasma must receive additional energy to prevent it from adiabatically cooling and falling back down to Sun (Klimchuk, 2012). The acceleration is a different physical step in the energization of the plasma, and could be from a different source than that which initially created the type II spicule.

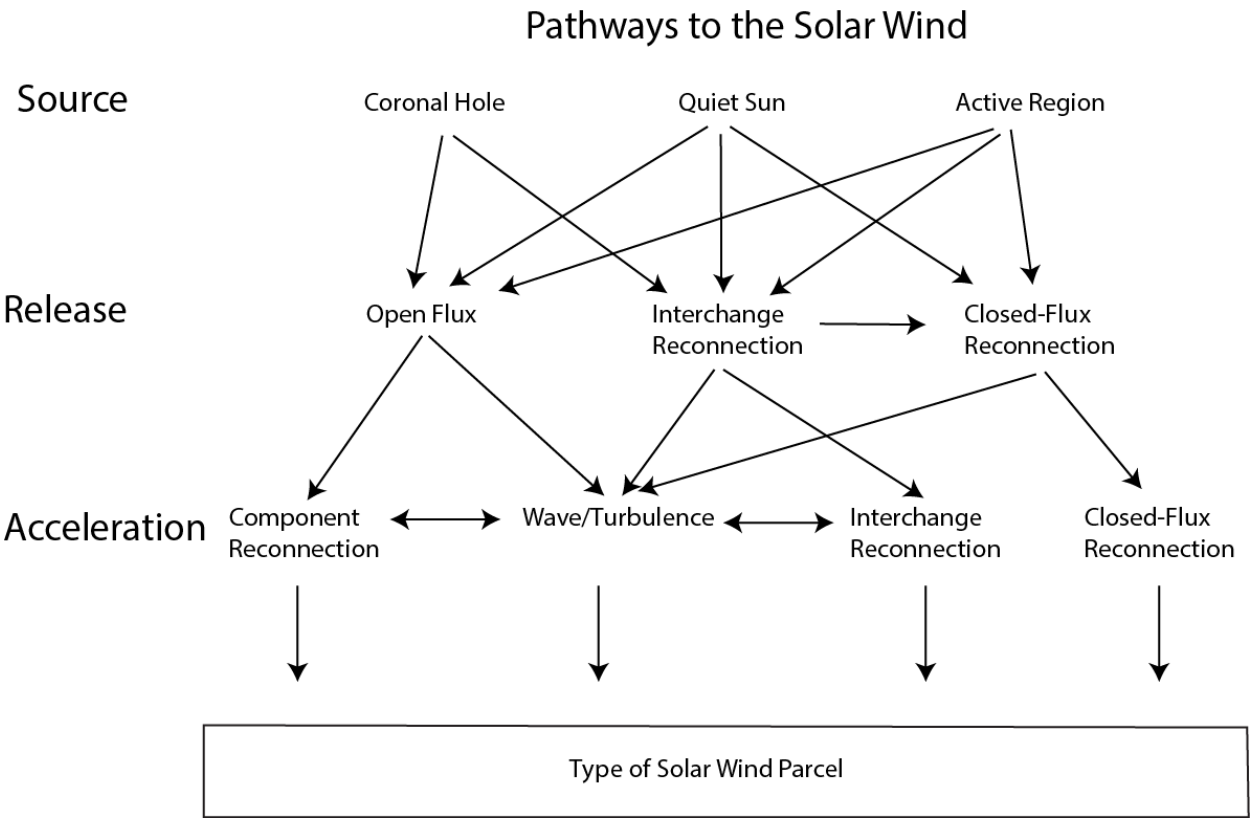

Figure 3 Pathways to the Solar Wind. Q1, source is the top line, there are three general options. Q2 is how the plasma parcel is released. Q3 is how the plasma is accelerated. The type of solar wind parcel that results will depend on which path it followed.

We show in Figure 3 the proposed new framework with multiple pathways to the solar wind. The framework separates the formation of the solar wind into three steps that correspond to the time history of the plasma parcel. The steps correspond to the three questions in this question group: (1) From where on the Sun does the solar wind originate? (2) How is the solar wind released? And (3) How is the solar wind accelerated? A significant difference from the old paradigm is that there is no presorting of the wind into fast and slow. Instead we now link the solar wind to qualifiers that correspond to the initial physical steps that the solar wind plasma parcel undergoes as it leaves the Sun. Separating the questions by these three steps is particularly

important if interchange reconnection is the release mechanism. In these cases, the initial state of the plasma (Q1) and the acceleration (Q3) occur on different flux tubes, and may be to be due to different physical mechanisms, or at least the mechanism operating in different physical regimes.

For convenience we conceptualize a parcel of solar-wind plasma near the Sun to be a mesoscale structure for which the frozen-in plasma properties of charge state, FIP abundance, and alpha/proton ratio are approximately homogenous. We return to frozen-in plasma properties in more detail in Question 4, and interpreting observations mesoscale structures in the solar wind in Question 5. A particular parcel of solar wind could have taken any of the paths in Figure 3. The goal is to determine how much each pathway contributes to the global solar wind, and under what conditions.

The new framework of Figure 3 does not imply that the three questions cannot be linked~~,~~ as they were in the historical paradigm of Figure 2. The point is that it is not a foregone conclusion that they are linked. The state of the global solar wind is determined by combining the statistics of all of the solar wind parcels. The four pathways from the historical paradigm are still contained within the new framework. For example, wind that comes from corona holes (Q1), along open flux (Q2), accelerated through wave turbulence (Q3) could produce fast wind in the same way that wave-turbulence produced fast wind from coronal holes in the historical paradigm. Open fields in coronal holes (Q1) can have local magnetic field concentrations, resulting in interchange reconnection, wherein reconnection releases the plasma (Q2), and accelerates the plasma (Q3). Figure 3 indicates the many new possible paths to solar wind in the new framework to explain solar wind observations that did not fit the historical framework. We discuss each physical step (question) in more detail in Sections 2.1, 2.2, and 2.3.

2.1. Question 1: *From where on the Sun does the solar wind originate?*

To scientists outside the solar wind community, it is surprising that the location on the Sun from which the slow wind originates is unknown. (Solar wind researchers might be likewise surprised to know that the magnetospheric community does not know what powers the aurora (Borovsky et al., 2020).) From where does the solar wind originate is a fundamental physics

question that impacts how the Sun and stars get rid of stressed magnetic fields, and is important for true predictability of the solar wind environment.

All solar wind originates from the solar corona, the atmosphere of the Sun. The solar corona can be separated into three broad categories: active regions (AR), quiet Sun (QS), and coronal holes (CH). These are measured in remote observations based on their radiative output and temperatures, which themselves are determined by the solar atmospheric heating, i.e. the so-called coronal heating problem. Active regions are the hottest and densest, and therefore brightest in EUV and X-ray emissions, while coronal holes are the coolest and most tenuous, and therefore dimmest in EUV and X-ray emission. Quiet Sun regions fall in the middle in terms of temperatures, densities and emission. The strength and topology of the magnetic field is different in each, and determines the coronal heating, or how much thermal energy is deposited to the plasma. Note that streamers, which were part of the original framework, are not explicitly named here. Streamers can be associated with either AR or QS magnetic field, and therefore the state of the plasma and the atmospheric heating within streamers will be dependent on the underlying magnetic field.

Note also that the term ‘coronal hole’ is sometimes used synonymously to mean ‘locations where field lines are open to the heliosphere’. Though coronal holes are generally associated with open field lines to the heliosphere, the correspondence between the brightness boundary determined in EUV measurements and the boundary between magnetically open and closed fields is not well-quantified (de Toma and Arge 2005). The corollary to this is how much magnetic flux is open to the heliosphere. The amount of open flux inferred from in situ magnetic field measurements are much larger than that estimated in coronal models driven by photospheric magnetic flux (Linker et al. 2017). Uncertainty in the correspondence of coronal hole EUV boundary detection methods (e.g. Krista & Gallagher, 2009; Caplan et al. 2016) with open flux still cannot account for the bulk of the discrepancy (Wallace et al. 2019), and it may be due to open flux at the poles that is likely systematically under-estimated (Tsuneta et al., 2008; Linker et al., 2017).

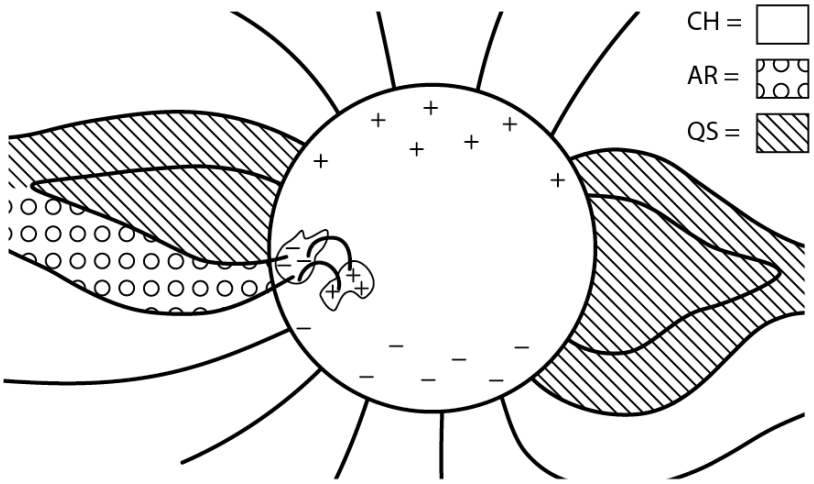

Figure 4 Cartoon of different source locations on the Sun, with black lines representing magnetic fields. An active region is present under the left streamer. The streamer on the left has plasma from the active region and plasma from the quiet Sun in it. The streamer on the right only has quiet Sun plasma.

We chose AR, QS and CH as the three options because the temperature and density is similar within each, suggesting a similar heating mechanism. However, there is some temporal and spatial variability within each type of source, indicating local changes in coronal heating, and it may prove useful to subdivide the sources. Examples of possible subdivisions in ARs are 'fan loops' located on the periphery of active regions, which are cooler and have a different FIP abundances than the cores of ARs, and AR age, since older ARs tend to be fainter in EUV and steadier than younger ARs (e.g. Ugarte-Urra & Warren 2012). The QS includes all locations of the closed-field corona without large enough concentrations of magnetic field to be ARs. Both newly emerged magnetic concentrations in the QS, and QS locations that are remnants of old ARs likely experience different coronal heating mechanisms than other locations of QS and are possible subdivisions. In CHs, a possible subdivision is between jets and their associated plumes, versus inter-plume locations. Jets and plumes are dynamic, brighter and hotter, suggesting a different coronal heating mechanism or manifestation than the inter-plume locations.

Excellent reviews about the origin locations for the solar wind (e.g. Feldman et al., 2005; Luhmann et al., 2013; Poletto, 2013; Cranmer et al., 2017) and the related question of coronal heating (e.g. Klimchuk 2015; Viall et al. 2020) can be found. Answering the question of the solar

342 locations of origin of different types of solar wind involves linking the flow of plasma and the
343 magnetic connectivity from the low corona through the high corona and out into the solar wind.
344 The atmospheric (coronal) heating that occurs leaves imprints in the resulting solar wind, which
345 we discuss in Q4 and Q5. The near-Sun observations of DKIST, Parker Solar Probe and Solar
346 Orbiter will be immensely valuable to the question of the origin location of the solar wind.

347

348 **2.2. Question 2:** ***How is the solar wind released?***

349 Once the initial state of the plasma parcel is determined (Q1), the next step in the life of a
350 solar wind plasma parcel is how the plasma gets out into the heliosphere, i.e. how it is released.
351 Put simply, is it already on a flux tube that is open to the heliosphere, or is reconnection required
352 to open up the flux tube? Figure 3 shows that plasma from all three locations on the Sun can be
353 released either through open flux or through reconnection. Reconnection of closed flux primarily
354 occurs at the HCS, which is the global polarity inversion line. (Note that explosive events such as
355 filament eruptions and coronal mass ejections involve closed-flux reconnection at their local
356 polarity inversion line, which does not have to be at the HCS).

357 Magnetic reconnection at the boundary between open and closed magnetic fields is
358 predicted to occur on many different spatial and temporal scales due to the complex, multiscale
359 evolution of the magnetic field (e.g. (Lionello et al. 2005; Rappazzo et al. 2012 Török et al. 2009;
360 Masson et al. 2014; Lynch et al. 2014; Pontin & Wyper 2015; Higginson et al. 2017a,b; Higginson
361 & Lynch 2018). On smaller scales, flux-replacement (recycling) estimates for the chromosphere
362 and corona vary from 1.4 - 3 hr (Close et al., 2004, 2005) to ~40 hr (Schrijver et al., 1997). On
363 larger scales, the equatorial extensions of coronal holes (associated with open fields) tend to exhibit
364 rigid rotation (e.g. Timothy et al., 1975; Adams, 1976; Hiremath and Hedge, 2013) in contrast to
365 the photosphere, which rotates differentially as a function of latitude; together, these observations
366 can be understood as the result of interchange reconnection (Nash et al. 1988; Fisk et al., 1999).

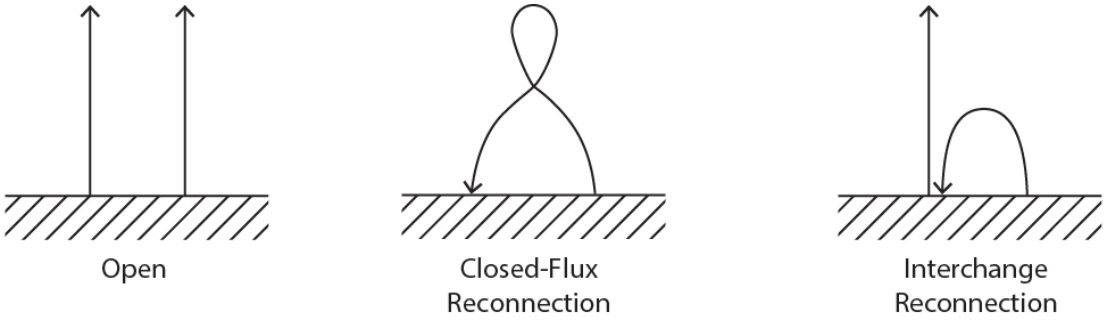

Figure 5 Cartoon of the three options for Q2 (How is the solar wind released?): open fields, closed-flux reconnection, interchange reconnection

The three general options for Q2 are illustrated in Figure 5 as a continuously open flux tube, closed-flux reconnection, and interchange reconnection. Closed-flux reconnection, or pinch-off at the helmet streamer (heliospheric current sheet) is predicted to have different magnetic field signatures than interchange reconnection at other locations along the open-closed boundary, with pinch-off (closed-flux) reconnection leading to flux ropes, and interchange reconnection leading to torsional Alfvénic fluctuations (Higginson & Lynch 2018). Pinch-off reconnection is the only reconnection that produces solar wind that is entirely magnetically disconnected from the Sun, indicated by an absence of the strahl. Pinch off reconnection does not have to disconnect the plasma entirely from the Sun if there is an axial magnetic field component still connected to the Sun; in fact, if both magnetic foot points remain connected to the Sun a bi-directional electron strahl can be present (Gosling et al., 1987). The height at which reconnection occurs might affect how much plasma escapes, and the gravitational settling signatures that survive into the heliosphere (Weberg et al. 2012).

Many observations indicate that interchange reconnection occurs at the edges of coronal holes (Baker et al., 2007; Subramanian et al., 2010; Krista et al., 2011), and generally at the open-closed boundaries (Owens et al. 2013; Owens et al. 2018; Sanchez-Diaz et al. 2016; 2017; Kepko et al. 2016; Mason et al. 2019). Reconnection is expected to produce time dynamics in the solar wind. Quasi-periodic trains of density structures (so-called ‘blobs’) are observed at helmet streamers (Rouillard et al. 2010a; 2010b; Sheeley et al. 2009; Wang et al. 1998; Viall & Vourlidas 2015; Viall et al. 2010). The in situ signatures of solar wind plasma near the heliospheric current sheet are also consistent with closed field plasma released through reconnection (Suess et al. 2009; Xu & Borovsky 2015) (see summary in the right column of Table 2): at 1 AU (1) the magnetic field in this type of plasma is statistically not Parker-spiral oriented, indicating it is not released

continuously, (2) the HCS plasma has an absence of an electron strahl, indicating that it lacks a magnetic connection to the Sun, and (3) when C^{6+}/C^{5+} is plotted as a function of O^{7+}/O^{6+} this HCS plasma follows the same pattern as ejecta does (cf. Fig. 10 of Xu and Borovsky (2015)), and not the pattern of the continuously emitted coronal-hole and streamer-belt plasma.

The web of separatrices (S-web) throughout the corona that defines the open-closed boundary is predicted to be dynamic, with magnetic fields opening and closing, pinch off as well as interchange reconnection occurring (e.g. Antiochos et al. 2012). Bright helmet streamers and pseudostreamers seen in EUV and white light observations of the solar corona are observational examples of the manifestations of the open-closed boundary. The S-web is subject to dynamics and reconnection from driving from the photosphere or from instabilities. Pseudostreamers and null point topologies are examples of S-web arcs that are observed to reconnect and release plasma into the heliosphere (Mason et al. 2019; Stansby et al 2018; Di Matteo et al. 2019). The magnetic-field concentrations from active regions are often involved in the creation of S-web arcs, and there are observational signatures of interchange reconnection associated with ARs (Del Zanna et al. 2011). However, it could take more than one reconnection exchange of plasma for the AR plasma to access open field lines and the heliosphere (Mandrini et al. 2014). We indicate such a series of reconnection events with a horizontal arrow from interchange reconnection to closed-flux reconnection in Figure 3 (pathways to the solar wind).

Coronal hole jets are another example in which reconnection events occur between localized concentrations of closed magnetic flux within open field coronal holes, and release mass into the solar wind (see reviews by Innes et al. (2016), and Raouafi et al. (2016)). Microstreams (Neugebauer et al 1995, 1997), which are observed in the fast wind associated with polar coronal holes, have velocity fluctuations of +/- 35 km/s and last 6 hours or longer in the solar-wind time series at 1 AU. They are thought to be the in situ signature of these reconnection jets (Neugebauer, 2012) due to the compositional changes and large angle magnetic discontinuities associated with them. Similar ~6-hr structuring is seen in the properties of the proton plasma and in the Alfvenicity (Borovsky, 2016). Velocity spikes seen in Helios data close to the Sun may be related phenomena (Horbury et al. 2018). Simulations support the connection between coronal hole jets and microstream/Alfvén waves (Karpen et al. 2017).

See Cranmer et al. (2017) and Rouillard et al. (2020) for excellent recent reviews of release mechanisms involved in the formation of the solar wind. The distinguishing observables for Q2 can be generally summarized as changes in plasma and magnetic field properties, because reconnection is an inherently time-dynamic process that produces parcels of solar wind with different plasma properties from each other and from surrounding wind produced in other ways. Time-stationary, open flux tubes can create solar wind parcels (structure) in the heliosphere as well. Solar rotation will rotate these different sources past an in situ spacecraft or planet, leading to changes in the in situ plasma, as the different solar wind streams advect past the spacecraft. This time/space ambiguity can be addressed in remote images or with multipoint in situ measurements. We return to this topic in Q5 'What is the origin and evolution of the mesoscale plasma and magnetic-field structure of the solar wind?'. In the future it will be important to have time dependent modeling of the corona and solar wind that captures the dynamics necessary to produce the different types and timescales of reconnection-released solar wind.

2.3. Question 3: *How is the solar wind accelerated?*

The third step in the life of a solar wind parcel is its acceleration to the terminal speed it reaches in the heliosphere. It is well known that a heated corona on open magnetic-field lines will produce a supersonic solar wind (Parker 1958). An important point is that in the Parker solar wind solution, the plasma is held at a constant temperature, and not allowed to cool adiabatically, and so implicitly assumes energy deposition as the plasma flows away from the Sun. The goal now is to figure out what that energy deposition mechanism is. It has been 60 years since the Parker solution, and we know that the kinetic physics involved in two-fluid solutions is likely important. Especially in the fast wind, electron conduction and heating of protons is necessary to get the very high speeds observed of 800 km/s. However, there are a number of unsolved issues about the acceleration of the solar wind: (1) how much does reconnection directly energize the solar wind (2) how is the Alfvénic turbulence cascade initiated and how is it dissipated (damping, parametric decay, phase mixing, and ion cyclotron waves), and (3) what is the role of the electron-driven ambipolar electric field.

In the new framework, acceleration could be directly tied to Q1, the heating occurring in the lower corona. This will be true for the case of a time-stationary, open flux tube with waves and

turbulence (e.g. Velli 1993). In this acceleration, the amount energy deposited below or above the sonic transition point determines whether the energy is deposited as heat or flow energy, and is related to the expansion of the magnetic field. Empirical studies showed that this 'expansion factor' is correlated with the wind speed (Wang et al. 1990), and may be evidence of wave/turbulence acceleration. Likewise, the reconnection that releases the plasma (Q2) could also provide all of the acceleration energy to the plasma, in which case Q2 and Q3 are linked. Empirically, distance from the coronal hole boundary is also correlated solar wind speed (Riley et al. 2015), which may be evidence of reconnection acceleration. However, Q1, Q2, Q3 are not necessarily directly connected. We illustrate this in Figure 3 and Figure 6. If the answer to Q2 is magnetic reconnection, then it may not be until the plasma is on the open flux tube that it experiences the physics that produces acceleration.

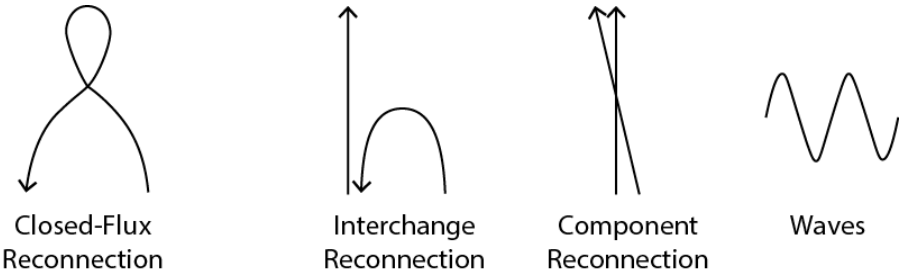

Figure 6, Q3 (How is the solar wind accelerated?), cartoon of the four different mechanisms of acceleration. Closed-flux reconnection, interchange reconnection, component reconnection, and wave/turbulence heating.

Reconnection may release plasma (Q2) but not provide much direct energization of the wind, in which case the reconnection is crucial for Q2, but not important for Q3. Conversely, component reconnection may be occurring in the open fields of coronal holes (Tenerani et al. 2016). This reconnection would not be important for plasma release (Q2), since the reconnection is between two open field lines, but could play a role in accelerating the solar wind (Q3). Horizontal lines in Figure 3 on the acceleration row indicate that waves can lead to reconnection and vice versa, and both can be involved in the energization of the plasma.

It is inevitable that ambipolar electric fields will contribute to the acceleration of the solar wind. Indeed, there is evidence that the slow wind continues to accelerate beyond Mercury (Schwenn et al., 1981; Arya and Freeman, 1991) as the electron heat flux decays with distance from the Sun (Stverak et al., 2009). Because of the vastly different parallel-to-B mobilities of low-mass electrons and high-mass protons, on open field lines there must be an ambipolar electric field

that retards the outward motion of electrons from the Sun. This ambipolar electrostatic field is the core of exobase models of the solar-wind evolution (e.g. Pierrard et al., 2004; Lemaire, 2012) where an interplanetary electric field acts to accelerate solar-wind protons outward at the expense of an electron pressure gradient (Lie-Svendsen and Leer, 2000; Meyer-Vernet et al., 2003). An analogous ambipolar electric field also exists in the outward "polar wind" from the high-latitude ionosphere of the Earth: in this case the situation is well diagnosed with in situ spacecraft measurements and there is no doubt that the ambipolar field is present (Winningham and Gurgiolo, 1982; Yau et al., 2007) and the outward-accelerated ions from this electrostatic field are observed (Haaland et al., 2012; Welling et al., 2015). The observation of weak electrostatic double layers in the solar wind (Mangeney et al. 1999; Lacombe et al, 2002) has strong implications for solar exosphere models: as pointed out by Borovsky and Gary (2014), double layers (which move with respect to the plasma) can be much more efficient at transferring momentum to ions (and heating the ions) than the static (non-moving) potential structure assumed in the existing exosphere models.

There are at least two distinctly different types of "slow wind", here denoted as the "Alfvénic slow wind" (D'Amicis et al., 2015, 2019) and the plasma associated with the sector-reversal region around the heliospheric current sheet, which is accelerated to even slower speeds, and often called the "very slow wind" (Sanchez-Diaz et al., 2016). This may indicate different acceleration mechanisms at work. The wind at the heliospheric current sheet is also sometimes called "streamer-stalk wind" (Susino et al., 2008), due to the fact that the heliospheric current sheet is directly tied to helmet streamers observed in white light images, though precisely which part of the streamer reconnects is still under active investigation, and is part of Q2. In Table 2 the properties of the two types are compared. Charge state measurements, which are an indication of the acceleration history (see description in Q4) are different for the two types of slow solar wind (Xu and Borovsky, 2015).

One hint about acceleration mechanisms (and source regions) lies in the fact that corotating interaction regions (CIRs) and the trailing edges of high-speed streams exhibit both gradual changes and abrupt changes in the plasma flow velocity, the proton specific entropy, and the heavy-ion charge states (Borovsky and Denton, 2010, 2016a). The CIR stream interface between coronal-hole (fast) wind and streamer-belt (slow) wind is often very sharp and very distinct, with

the Alfvénicity of the plasma transitioning at 1 AU in an hour or two. If the "Alfvénic slow wind" was the result of a mix of mechanisms, that should result in a gradual shift in the Alfvénicity. If the Alfvénic slow wind plasma were caused by a speed-versus-expansion relation, indicating wave/turbulence acceleration, with increasing flux expansion at the edge of the coronal hole, that should result in only gradual speed transitions from little expansion at the center of a coronal hole to the highest expansion in the slow wind. Particularly if the velocity measurements are rotated into a local-Parker-spiral coordinate system, the stream interface exhibits a strong abrupt change in the flow velocity along the Parker-spiral direction (a vorticity layer).

Table 2. A comparison between streamer-belt-origin plasma (Alfvénic slow wind) and sector-reversal-region plasma (streamer-stalk wind).

Property	**Alfvénic slow wind**	**Sector-Reversal-Region Plasma**
Speed	Slow	Very Slow
Proton Specific Entropy	Medium	Very Low
Alfvénic	Yes	No
Parker-spiral-field orientation	Yes	No
α/p density ratio	Normal	Very Low
Inhomogeneous	Yes	Very
Strahl	Yes	No
C^{6+}/C^{5+} versus O^{7+}/O^{6+} pattern	Like Coronal-Hole Plasma	Like Ejecta

Modeling capabilities of the solar wind continue to improve; see MacNeice et al. 2018 for a recent review. Solar wind models that include multifluid effects are now coming online (Ofman et al. 2015; Usmanov et al. 2018), which is important for understanding the evidence of ion-cyclotron energization (Cranmer 2009). Additionally, the details of the magnetic topology can greatly affect acceleration, and are important for understanding. Magnetic funnels at pseudostreamers are one example of such magnetic field topologies (Panasenco et al. 2019). The Air Force Data Assimilative Photospheric Flux Transport (ADAPT) model is a sophisticated surface flux transport model which assimilates full disk magnetograms on an hourly timescale [Arge et al. 2013; Hickmann et al. 2015], and is the current state-of-the-art in providing observed time dependent global surface field input to coronal models, which can then be used to drive the solar wind (e.g. Linker et al. 2016).

Applying the new framework

Table 3. Physical questions for each step in the pathway to a solar wind parcel. Theories and options for each question (first row) with distinguishing observations and indicators (second row), separated by signatures that are only valid close to the sun and those that are conserved and can be used throughout the heliosphere. The third row indicates how each physical step has a space weather impact.

Physical Questions	Q1: From where on the Sun does the parcel of solar wind originate?	Q2: How and at what height was it released to the Heliosphere?	Q3: How was it accelerated?
Categories of theories	coronal hole; active region; quiet Sun	reconnection; continuously open field	reconnection energization; waves/turbulence
Distinguishing observational signatures	near Sun only: flow tracks in images; T conserved quantities: FIP; alpha/proton; heat flux intensity; specific entropy*	near Sun only: flow tracks in images; flux ropes; changes in T; changes in T_{par}/T_{perp} conserved quantities: heavy ion dropouts; abundance of sulfur; composition changes (FIP or alpha/proton) that occur with changes in magnetic field, heat flux, or density; specific entropy*	near Sun only: velocity; T; T_{par}/T_{perp}; T_{ions}; Alfvénicity conserved quantities: alpha/proton; charge states; specific entropy*
Space weather contribution to the Heliosphere.	mass; magnetic flux	structure; variability; helicity	flow energy; stream interaction regions

We summarize the new framework for understanding the formation of the solar wind in Table 3. The headers are the three questions from this overarching theme. The first row lists the theoretical categories to explain each physical step, described above in their respective questions. The second row lists the observational signatures to distinguish between the theoretical categories, separated into those that are conserved and can be used in in situ measurements throughout the heliosphere, and those that can only be used close to the Sun e.g. in remote images and the in situ measurements of Parker Solar Probe, Helios and Solar Orbiter. Specific entropy has an * to

545 indicate that it actually is not a conserved quantity, but is correlated with those that are; we revisit
546 this and the other conserved quantities in Q4. The ultimate goal is to determine how much solar
547 wind each of the possible theories contributes to the heliosphere and how that varies with solar
548 cycle. The third row lists the aspect of each step of formation that is important for space weather,
549 both in terms of impact on planetary bodies, as well as in forming the medium through which
550 ICMEs and energetic particles propagate through.

551 For Q1, the main observable near the Sun that may be able to distinguish between AR,
552 CH, and QS plasma is flows in remote imagery that have coverage from the low corona up
553 through to the solar wind. Flows can be measured using optical flow tracks or mass flux
554 estimates (e.g. DeForest et al. 2018), doppler dimming of spectral lines (Bemporad 2017), or
555 white light filters at temperature and speed sensitive wavelengths (Reginald et al. 2018).
556 Coverage from the low corona to the high corona is crucial for this question. Such a combined,
557 continuous field of view coverage with adequate time coverage and resolution to track flows
558 from the low to high corona is rare, due to instrumentation limitations. EUV and X-ray emissions
559 are dependent on density squared, and so images of the corona in those emissions fall rapidly
560 with height above the photosphere. White light coronagraph images are subject to strong
561 scattering, making their relative noise increase in the low corona. Temperature measurements
562 very close to the Sun, especially in combination with flow tracks, are also an indicator of source,
563 since active regions can be several times hotter than coronal hole plasma. Observables that are
564 conserved quantities and can be used throughout the heliosphere are FIP abundances,
565 alpha/proton ratios, heat flux intensity (the strahl) and specific entropy.

566 From where the solar wind originates determines how much solar wind mass and
567 magnetic flux fills the heliosphere and where in the heliosphere each type of wind goes are
568 important pieces of information for space weather. For this question, coronal holes are already
569 agreed upon to be a major contributor. The relative contribution of QS and AR plasma is the
570 remaining uncertainty. Additionally, there are times in the solar cycle at which there are no
571 active regions on the Sun, and so only QS and CH wind is possible.

572 For Q2, the observables that may be able to distinguish between magnetic reconnection or
573 continuously open field lines near the Sun are flow tracks in images, flux ropes, changes in
574 temperature, and changes in Tpar/Tperp. Flow tracks for answering Q2 have similar benefits and
575 challenges to those described for Q1. In this case, in-out pairs of flows indicate magnetic

reconnection, and the height of reconnection can be localized in the images. Flux ropes are a consequence of reconnection; however, they can also be made at the HCS in the heliosphere. Further from the Sun, flux ropes in conjunction with a conserved quantity indicates reconnection as the release mechanism. Temperature and temperature anisotropy changes to the plasma are expected if reconnection releases the plasma. Of the conserved quantities, heavy ion dropouts, which indicates gravitational settling and is a unique indicator of the height at which reconnection occurred. For reasons described in Q4, sulfur may be a unique indicator of plasma from closed field lines that then undergo reconnection. The other conserved quantities that indicate reconnection released wind are FIP abundances, specific entropy, and alpha/proton number-density ratios, particularly when they change in conjunction with changes in magnetic field, heat flux, or density. Waves across plasma boundaries, such as Kelvin Helmholtz at the HCS, which could also produce correlated magnetic field changes with compositional changes, are theoretically possible. In such cases, the magnetic field rotations have a precise relationship with composition and plasma boundaries, and can easily be identified or ruled out (Crooker et al. 1996).

The space weather contribution to the heliosphere is how much structure, variability, and helicity is created through each type of release. If reconnection occurs and results in flux ropes, helicity could also be injected. Taking coronal hole jets as an example, the presence of microstreams is an indication of the variability that the jets contribute to the heliosphere. As for the mass that the jets contribute, observational estimates range from mass 10% of solar wind (Cirtain et al. 2007), to 4% (Young 2015), to 3.2 % (Jackson et al. 2004); Lionello et al. (2016) used MHD simulations to estimate the contribution of the jets and concluded that coronal hole jets contribute 0.4–3.0% of mass to solar wind. As another example, helmet streamer-tip reconnection wind can only fill the region of the heliosphere immediately adjacent to the HCS. Yet slower solar wind is observed at 30 degrees and more above the HCS (Burlaga and Forman 2002), a much larger volume than streamer-tip reconnection can account for. The predicted S-web arcs allow such a large solid angle (volume) of slow wind into the heliosphere (Titov et al., 2011; Crooker et al., 2012), and observations of reconnection-released plasma far away from the HCS support this (Stansby et al. 2018; Di Matteo et al. 2019).

For Q3, the observables that may be able to distinguish between acceleration theories near the Sun are velocity, temperature, and temperature anisotropies, ion temperature, and Alfvénicity. Conserved quantities that can be used throughout the heliosphere are alpha/proton

ratios, charge states of heavy ions, and specific entropy. The space weather contribution is the dynamic pressure from the flow energy as well as the stream interaction regions formed between flows of different speeds.

We stress that Table 3 is based on the state of the field today, and we have every expectation that with DKIST, Parker Solar Probe, Solar Orbiter, PUNCH, and modeling and theoretical advances, the community will provide new measurements and understanding that fill in this table more accurately.

Theme 2, Interpreting observations of solar wind parcels

In this group of outstanding questions, we discuss the two outstanding questions (Q4 and Q5) regarding the physics of the properties of the solar wind and how to interpret the plasma signatures of solar wind plasma parcels. We provide the rationale for the defining observables presented in Table 3, namely that some quantities in the solar wind evolve as the solar wind advects outwards, while others are conserved, and are imprints of coronal heating and solar wind formation. Some aspects of what determines the conserved plasma signatures are understood, while others are not.

2.4. Question 4: *What determines the heavy-ion elemental abundances, the ionic charge states, and the alpha/proton density ratios in the solar wind? (And what do they tell us about the Sun?)*

As a solar wind parcel advects through the heliosphere, it experiences expansion, compression, rarefaction, wave-particle interactions, instabilities, reconnection, etc., which alter its density, temperature, velocity, heat flux and magnetic field. Ionic charge states, the abundance enhancement of elements with low FIP (first-ionization potentials), and the alpha/proton density ratio follow well-known trends. Ionic charge states are inversely correlated with solar wind speed (cf. Table 2 of Borovsky, 2012c), such that slower winds are associated with higher charge states, and faster winds are associated with lower charge states. FIP abundances follow a trend with slow wind having enhanced abundances of low-FIP elements and fast wind having only a slight enhancement of low-FIP elements (Pilleri et al., 2015). Elements with a FIP below about 10 eV, such as Mg Si and Fe, are low FIP, while elements with a FIP above 10 eV, such as O, Ne and He, are high FIP. Alpha-to-proton number-density ratios are positively correlated with solar wind speed (Ogilvie & Hirshberg, 1974; Kasper et al., 2007). The abundance of heavy elements in general increases during solar maximum and decreases during solar minimum, but in proportion to each other so that the relative FIP patterns are not solar cycle dependent. The solar wind ionic charge states are higher (hotter) towards solar maximum (Lepri et al., 2013) and over a solar cycle the global alpha/proton number-density ratio increases during solar maximum (Kasper et al., 2012).

Spectroscopic measurements show that the ratio of number densities of low FIP to high FIP elements is higher in the corona relative to the photosphere; this enhancement is small in coronal holes and fast wind, and larger in the slow wind and closed-field areas of the solar corona (Feldman and Widing, 2002; Heidrich-Meisner et al., 2018). The overabundance of elements with low first ionization potential is set in the chromosphere (Peter, 1998). A thorough description of the possible physical mechanisms at work is reviewed by Laming (2015). The chromosphere has substantial populations of both ions and neutrals, due to its relatively low temperatures. This is in contrast to the mega-Kelvin corona where the plasma reaches a highly ionized state. When plasma is in the partially-ionized chromosphere, elements with low FIP will be preferentially ionized while high-FIP elements will still be neutral. Electromagnetic forces act on the ionized species and not

the neutral species, leading to an elemental fractionation with an overabundance of low-FIP ions transported from the chromosphere into the corona. For plasma on field lines open to the heliosphere, this elemental fractionation is 'frozen in' to the plasma, i.e. it remains unchanged as it fills the corona and advects with the solar wind. A closed loop in the corona has FIP elemental abundances that are time dependent, as cycles of coronal heating and cooling and associated mass exchange with the chromosphere occur. In new theoretical work extending our understanding of the FIP effect (Laming et al., 2019), sulfur seems to be a key for Q2 about the release of the solar wind from the corona (as noted in Table 3), due to its first ionization potential being between high-FIP and low-FIP elements. The result is that sulfur can behave as either a low or high FIP element, depending explicitly on whether or not the flux tube is open to the heliosphere. Based on measurements of the abundance of sulfur, the average solar wind exhibits evidence for a mixture of solar wind from both open and closed fields (Laming et al. 2019).

Ionic charge states are determined by (1) electron temperatures, (2) electron number densities, and (3) the amount of time the ions spend with the electrons. The timescale for heating the high hot (1-2 MK) closed loops is in the range of 1 - 6 hr (Sheeley, 1980; Kopp et al., 1985; Viall and Klimchuk, 2017; Reale, 2014). The timescale for carbon and oxygen to reach charge-state equilibria by progressive ionization in the hot (1-2 MK) high loops is in the range of 10^4 s (for $n_e = 10^8$ cm^{-3}) to 10^6 s (for $n_e = 10^6$ cm^{-3}) (cf. Fig. 1 of Smith and Hughes (2010) or Fig. 3 of Landi et al. (2012a)). To a large degree the ionic charge states are set by the electron temperature at the height at which the charge states are frozen in, which is the height at which the plasma flows away from the Sun fast enough in low-enough electron density so that the charge states no longer evolve. This is because charge-state evolution is faster at lower altitudes where the electron density is higher, and the evolution is very slow at higher altitudes where the electron density is low. Traditionally, since loop height corresponds to the electron temperature, the solar wind ionic charge-state ratio was related to loop height (Feldman et al., 1999; Gloeckler et al., 2003). While the FIP abundances are set in the chromosphere before the heavy ions reach the corona, the ionic charge states are set a solar radii or more above the photosphere; this is a greater height than most coronal loops reach. Landi et al. (2012b) showed the charge-state freezing in typically occurs at heights of 1.5 and 3.0 solar radii above the photosphere. Oran et al. (2015) showed that most, but not all of the observed charge states can be reproduced with time-stationary open fields. Therefore

687 (cf. Table 3), charge state is a tracer of Q3 (acceleration) and possibly Q1 (the initial thermal state)
688 but not likely a direct test of Q2 (release).

689 The solar wind alpha-particle abundance relative to protons probably has its roots in part
690 in the fractionation processes in the partially-ionized chromosphere (Peter and Marsch, 1998), with
691 helium having the highest FIP of any element. In the solar wind, the alpha/proton number-density
692 ratio is positively correlated with wind speed (Ogilvie and Hirshberg, 1974), however in coronal-
693 hole-origin solar wind observed at 1 AU, that correlation is weak. The ecliptic alpha/proton
694 number-density ratio increases during solar maximum (Kasper et al., 2012); some of this
695 alpha/proton solar-cycle variation can be explained by the prevalence of ejecta plasma and absence
696 of sector-reversal-region plasma in the ecliptic during solar maxima, with ejecta having high
697 alpha/proton ratios and sector-reversal-region plasma having very low ratios (Xu and Borovsky,
698 2015). The alpha/proton density ratio exhibits sudden changes across magnetic discontinuities in
699 the solar wind (Borovsky, 2020b): since a boundary in the alpha abundance can only be created at
700 the Sun, measurements of the alpha/proton density ratio in the solar wind are potential tracers of
701 flux-tube dynamics at the Sun (cf. Table 3). (The abundances and charge states of heavy ions might
702 also exhibit sudden changes across magnetic discontinuities, but the time resolution of current
703 heavy-ion data sets is too poor to determine this.) In the heliosphere the alpha particles move
704 outward from the Sun faster than the protons (Asbridge et al., 1976; Marsch et al., 1982), traveling
705 with the mesoscale magnetic structure rather than with the proton plasma (Nemecek et al., 2020).
706 The differential flow between the alphas and protons is proportional to the bulk velocity (Steinberg
707 et al. 1996). This proton-alpha velocity difference may provide clues to the mechanisms that
708 accelerate the solar wind.

709 The proton specific entropy $S_p = T_p/n_p^{2/3}$ of the solar wind follows similar trends to that of
710 charge states; the proton specific entropy is correlated with speed and anticorrelated with heavy-
711 ion charge states (Pagel et al., 2004). The proton specific entropy has been used as an identifier of
712 solar wind at 1 AU (Xu and Borovsky, 2015; Camporeale et al., 2017). However, proton specific
713 entropy is not a conserved quantity (Freeman, 1988) and it evolves with distance from the Sun. It
714 is still unknown what mechanism(s) back at the Sun it is a proxy for, although (as noted in Table
715 3) it may provide useful high-time-resolution information for Q1-Q3, solar wind formation.

716 Reading the solar-wind time sequence data of FIP abundances, ionic charge states, and
717 alpha-to-proton density ratios yields clues to the time and space dependence of coronal structure
718 and processes (cf. Q1 and Q2 in Table 3). These properties are 'frozen in' and do not evolve with
719 distance from the Sun (but see Hollweg et al. 2014 and Durovcova et al. 2019 for particular
720 situations in which the alpha/proton ratio can be altered). The alpha streaming relative to protons
721 in the solar wind may hold cues to the acceleration mechanisms (Q3) of the solar wind. To exploit
722 this information, better understanding of the connection of these solar-wind measurements to
723 physical processes at the Sun is needed as well as higher-time-resolution, higher-accuracy solar
724 wind measurements of heavy ions and alpha particles.

725 As noted in Table 3, FIP elemental abundance relates to Q1 (location on the Sun) and Q2
726 (release). FIP abundances provide no direct information about Q3 (acceleration). Future high
727 temporal and spatial resolution sulfur measurements in remote spectroscopy off the limb, and
728 sulfur measurements in situ would be very useful (see Del Zanna and Mason 2018 for a thorough
729 review of spectral line measurements). Future models that include the crucial physics of
730 chromosphere-to-coronal transport to reproduce the FIP effect, simultaneously with dynamic
731 opening and closing of loops will be important for understanding how the timescales of release
732 effect the plasma parcel that is in the solar wind. For example, if the loop undergoes a new
733 reconnection event too rapidly after closing down, it may not have had time for fractionation to
734 occur.

735 The heavy ion abundance and alpha/proton density can generally be determined by the FIP
736 mechanism, but it could also be determined by gravitational settling (Raymond et al. 1997; Endeve
737 et al. 2005; Weberg et al. 2012). In principal in situ data can distinguish between these, but it
738 requires data from enough elements to sort by FIP and also by mass, which in practice exist, but
739 are rare. Alpha behavior in the corona is especially difficult to determine, due to the lack of spectral
740 lines (helium is fully ionized in the corona and so there are no electron transitions to image).

741 The alpha-to-proton density ratio provides the highest-time-resolution method to study the
742 magnetic structure of the corona using solar wind measurements (e.g. Safrankova et al., 2013).
743 Close-to-the-Sun alpha/proton measurements by Parker Solar Probe will greatly advance this
744 connection. Solar Orbiter will have heavy-ion abundance and charge-state measurements at much

745 higher time resolution than has been available so far, fast enough to differentiate boundaries of
746 individual flux tubes.

747

748 **2.5. Question 5:** ***What is the origin and evolution of the mesoscale plasma and magnetic-field***
749 ***structure of the solar wind?***

750 A major question concerns the structure and dynamics of the heliospheric plasma and
751 magnetic field and its connections back to the Sun. This relates to the relative roles of active MHD
752 turbulence, dead turbulence (turbulence that has exhausted its energy and left behind a structured
753 magnetic field), nonlinear Alfvén waves, advected pressure-balance structures, fossil coronal flux
754 tubes, magnetic holes, mirror modes, etc. (Neugebauer and Giacalone, 2010, 2015; Li and Qin,
755 2011; Owens et al., 2011; Tu et al., 2016).

756 Solar wind structure comes from three sources: (1) spatial structures on the Sun, plus the
757 solar rotation and the expansion of the wind away from the Sun, (2) time dynamics at the Sun,
758 including reconnection of magnetic fields, spicules, jets, etc., and (3) evolution in the heliosphere,
759 e.g. turbulence, which destroys structure originating from the Sun and continually creates and
760 destroys new structure. The question is what are the relative contributions of sources (1), (2), and
761 (3): when, where, and what do they look like. Very large scale structure with timescales of a day
762 or so (CIRs, high-speed streams, trailing edges, heliospheric current sheets, heliospheric plasma
763 sheets, CMEs, …) are created by identifiable magnetic and velocity features in the corona of the
764 rotating Sun. On mesoscales (timescales in the range of minutes up to a few hours), determining
765 the origin of the structure is difficult due to observational limits, modeling limits, and an
766 incomplete understanding of all of the competing physical processes that can act, making it
767 difficult to model the connection between the solar wind and the solar source. These mesoscales
768 are much larger than kinetic scales (microscales).

769 As the solar wind plasma advects past a spacecraft, fluctuations in all quantities at all
770 timescales are seen. At timescales of seconds and longer it is safe to assume that the temporal
771 fluctuations largely represent spatial structure of the plasma and magnetic field. There are robust
772 velocity and magnetic-field fluctuations in the plasma (with changes $\langle|\Delta\underline{B}|/|B|\rangle \sim 0.5$ and $\langle|\Delta\underline{v}|/v_A\rangle$
773 ~ 0.35 at 30-min timescales) and the estimated Reynold's numbers of these fluctuations are

extremely high (Borovsky and Gary, 2009), so it makes sense that the velocity and magnetic-field fluctuations are turbulence (Coleman, 1968; Matthaeus & Goldstein, 1982). Observed magnetic and velocity power spectral densities are consistent with expectations for MHD turbulence (Podesta et al., 2007; Perez and Boldyrev, 2010; Wicks et al., 2010; Boldyrev et al., 2011), and higher-order moment calculations are also consistent with dissipating turbulence (Hadid et al., 2017; Smith et al., 2018). Some solar wind statistical analyses aim to quantify the effects of "coherent structures" or "intermittent structures" in the statistical transformations of solar wind time-series data (e.g. Bruno et al, 1999, Salem et al., 2009; Greco et al., 2010; Bruno, 2019). Nonetheless there are issues as to the role of non-turbulent structures in the solar wind measurements. Analyses of turbulence in the solar wind are statistical analyses, typically in frequency space, and often without consideration of what specific types of structures (i.e. current sheets, plasma boundaries, magnetic holes, pressure-balance structures, mirror modes) are in the solar wind time series. As depicted in Figure 7, looking at the output of a statistical (e.g. Fourier or structure-function) analysis it is difficult to discern what was in the time series: e.g. magnetic decreases, pressure balance structures, flux ropes, plasma boundaries, plasma blobs, etc.

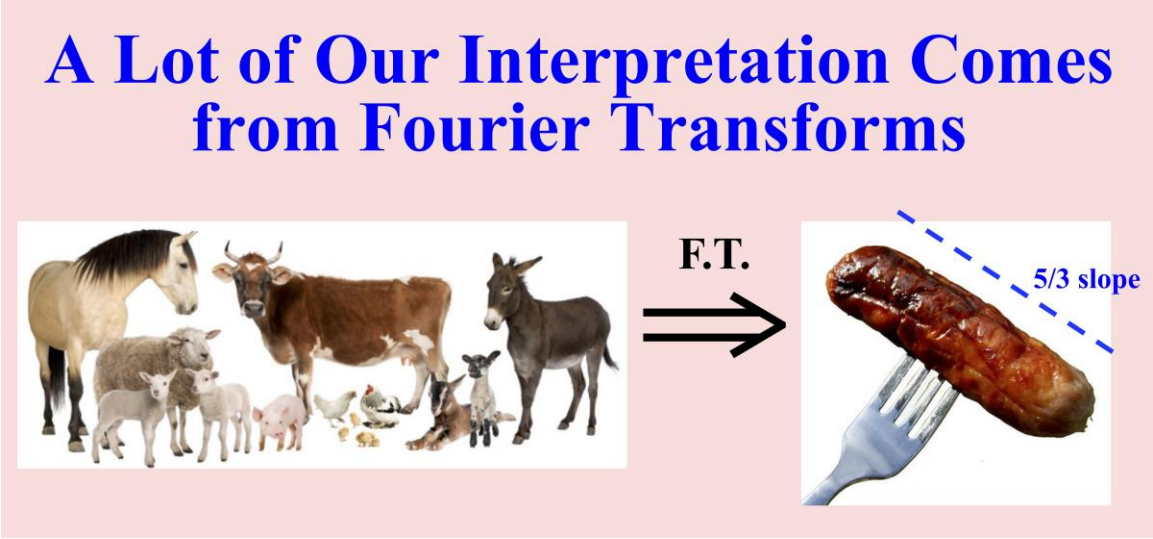

Figure 7. A comical depiction of the transformation (blending) of information from the solar wind time series (left) to a Fourier power spectrum or other statistical reduction (right).

Understanding the nature and dynamics of the mesoscale structure is important for the transport of energetic particles in the heliosphere, for the propagation and evolution of coronal

mass ejections, for processes at interplanetary shocks, and for solar heat-flux transport. The mesoscale structure of the magnetic field is largely structured into magnetic flux tubes (McCracken and Ness, 1966; Michel, 1967; Bruno et al., 2001). The origin of the flux-tube structure is debatable and probably mixed (turbulence, dead turbulence, solar coronal structure, Alfvén wave dynamics, etc.), but the high level of intermittency associated with coherent structure is not debatable.

The mesoscale structure of the solar wind is also an important part of the Sun-Earth connection (Borovsky, 2020c). The temporal changes in the magnetic field associated with the passage of flux tubes results in sudden changes in the rate of dayside reconnection and the driving of the magnetosphere: depending primarily to the local orientation of each tube, some flux tubes are geoeffective, some are not. Some flux tubes will be capable of driving a magnetospheric substorm (Freeman and Morley, 2009; Newell and Liou, 2011) as they pass. When the current sheets that form the walls of the flux tubes come into contact with the Earth's bow shock the current sheets can produce hot-flow anomalies upstream of the Earth (Schwartz et al., 2000). Ambient solar wind mesoscale structures also drive ULF wave dynamics in the magnetosphere (Kessel 2008; Wang et al. 2017). Large-amplitude (>2x) solar wind density structures produce sudden changes in dynamic pressure that compress and relax the entire magnetosphere, causing globally coherent compressional oscillations (Cahill and Winckler 1992; Korotova & Sibeck 1995; Matsuoka et al. 1995; Sarafopoulos 1995; Borovsky and Denton, 2016b). One type of mesoscale solar wind structure occurs as quasi-periodic enhancements of density optically observed at the Sun and throughout the inner heliosphere (Viall et al. 2009b; Kepko et al. 2016; Di Matteo et al. 2019) and detected in situ at the Earth's magnetosphere (Viall et al. 2008, 2010; Di Matteo & Villante 2018). The quasi-periodic dynamic-pressure enhancements drive globally coherent ULF waves inside the magnetosphere at the same frequencies (Kepko et al. 2002; Viall et al. 2009a): the ULF waves are observed by ground magnetometers (Villante et al. 2016), as radar oscillations in the high latitude ionosphere (Fenrich & Waters 2008), in polar UV imaging data (Liou et al. 2008), in the radiation-belt dynamics (Kepko & Viall 2019), and even the equatorial ionosphere (Dyrud et al. 2008). MHD simulations capture this interaction, and show that locations of field line resonance will even amplify the waves (Claudepierre et al. 2010; Hartinger et al. 2014). Finally, the current sheets of the solar wind are often the sites of strong (~80 km/s) wind shears that disrupt the Earth's magnetotail as they advect past (Borovsky, 2012a).

In the highly Alfvénic solar wind, variations in the proton flow vector and the magnetic-field vector seen by a spacecraft are highly time correlated with $\Delta \underline{v} \approx \pm \Delta \underline{B}/(4\pi\rho)^{1/2}$: the changes in $\underline{v}$ are parallel (or antiparallel) to the changes in $\underline{B}$. This means that if you shift into the reference frame that moves with the magnetic structure, you see a network of flux tubes, with each flux tube having a parallel proton plasma flow inside of it at a fraction of the Alfvén speed (Borovsky, 2019a). The correlations are such that the plasma flow relative to the structure is toward the Sun, hence the structure is moving outward along the Parker spiral relative to the proton plasma at a fraction of the Alfvén speed. In the reference frame of the magnetic structure, the flow is everywhere parallel to the magnetic field; any plasma flow velocity perpendicular to the local magnetic field is below the noise of the measurements. This includes the very large velocity shears across the current sheets at the flux-tube walls: the rotating plasma flow is parallel to the rotating magnetic field. This lack of a perpendicular-to-$\underline{B}$ flow in the reference frame of the magnetic structure indicates that the magnetic structure is not evolving as it moves outward from the Sun. (Nemecek et al. (2000) refer to the frame that move outward with the magnetic structure as the de Hoffmann-Teller frame of the solar wind: they find that the alpha particles of the solar wind tend to move with this frame.)

Some clues to the nature of the non-turbulence mesoscale structure of the solar wind are the following. (1) Solar wind flux tubes can have a long-distance coherence from the Earth to near the Sun (Gosling et al., 2004; Trenchi et al., 2013; Borovsky, 2020b). (2) Some flux-tube walls are also plasma boundaries (e.g. they exhibit changes in the proton specific entropy, the density, the ionic composition, the field strength, the electron heat flux, and the plasma β) (Borovsky, 2008; Borovsky, 2020b). (3) Tube cross sections squash and stretch under the action of compression (CIRs) and rarefaction (trailing edges), respectively: the statistical amount of squashing and stretching matches theoretical predictions for static structures (Borovsky and Denton, 2016a). (4) In the Alfvénic solar wind in the reference frame of the magnetic structure, there are parallel plasma flows in each flux tube, with the flow vector changing from tube-to-tube because the field direction changes from tube-to-tube. (5) There is a lack of evidence of turbulent mixing in the slow solar wind (Borovsky, 2012b). (6) Some solar wind structures survive from the Sun to 1 AU. One example of surviving structure is the periodic density structures imaged at streamer stalks (Viall & Vourlidas, 2015) and detected upstream of Earth's magnetosphere (Kepko & Viall, 2019). A second example is the narrow (~10^4 km at 1 AU) CIR stream interface between fast and slow wind

856 (Borovsky, 2006), whose thickness is consistent with Bohm diffusion acting over the ~100-hr
857 lifetime of the solar wind plasma advecting from the Sun to 1 AU.

858 White light images provide important information regarding two sources of mesoscale
859 structures: coronal structure versus turbulence evolution. Mesoscale structures coming directly
860 from the upper corona as the solar wind is formed are observed using STEREO/SECCHI HI1 white
861 light imaging (FOV is 15-90 Solar radii); and as the solar wind advects out, turbulent fluctuations
862 on mesoscales appear in the images, which coexist with the mesoscale structures that came directly
863 from the Sun (DeForest, et al. 2016). In rare circumstances, mesoscale structures can be followed
864 from their release at the Sun, through the heliosphere, to Earth impact in the STEREO/SECCHI
865 heliospheric imagers (Rouillard et al. 2010a; 2010b; 2010c). However, the direct Sun-Earth
866 connection in white light is biased to mesoscale structures with density enhancements (white light
867 image intensity is proportional to the electron density). Additionally, current heliospheric imagers
868 are resolution and noise limited, and most mesoscale structures fall below the noise floor well
869 before they get to Earth. Lastly, though distinguishing the development of dynamics en route from
870 solar structures is relatively straightforward in imaging data, using ecliptic-viewpoint
871 measurements it is however difficult to tell (a) time stationary spatial structures from the Sun from
872 (b) time dynamic released structures. A polar is view is better suited, since the line of sight is
873 parallel to the rotational axis of the Sun. Solar Orbiter's extended phase with its 30^{o} orbit
874 inclination will get a peek. For understanding the origin of mesoscale structures impacting the
875 Earth, we are currently limited to single point, in situ measurements, with a few rare intervals with
876 multi spacecraft measurements (e.g. Thieme et al., 1989). In situ measurements of plasma
877 parameters of mesoscale structures at distributed longitudes upstream of Earth could decouple
878 solar sources (a) and (b) due to the rotational offset in longitude expected for structures from source
879 (a).

880 Excellent reviews of the issues associated with mesoscale structure can be found (Schatten,
881 1971; Neugebauer and Giacalone, 2010; Owens et al., 2011, Bruno and Carbone, 2013, 2016).

882 Future progress will be helped by higher sensitivity and resolution white light imagers,
883 such as those of PUNCH, and by higher-accuracy higher-time-resolution measurements of the
884 magnetic field, plasma flow, heavy ions, and electron strahl. Investigations of strahl statistics can

reveal details of the magnetic-field structure between the Sun and the measuring spacecraft. Innovative methods to trace field lines in the solar wind could be greatly helpful.

Theme 3, Physical mechanisms operating on solar wind formation and evolution

In this group of questions, we discuss the four outstanding questions (Q6-9) regarding the physical mechanisms that operate on solar wind formation and evolution. Answering these questions involves understanding fundamental physical processes. These processes change the solar wind plasma and particle populations as the solar wind advects outward and provides the rationale for the defining observables that are not conserved in Table 3.

2.6. Question 6: *What is the Origin of the Alfvénic Fluctuations in the Solar Wind?*

In fast coronal-hole-origin plasma, and to a lesser degree, in intervals of slower speed wind, the fluctuations are dominated by outward-propagating Alfvénic fluctuations (Belcher and Davis, 1971; D'Amicis et al., 2019) with strong correlations between the vector changes $\Delta\underline{v}$ and $\Delta\underline{B}$. Strong Alfvénic fluctuations are also observed in the transition region and corona (McIntosh et al., 2011). In the solar wind the Alfvénic fluctuations are seen on timescales from seconds to days. The Alfvénic correlations are particularly strong across strong current sheets (directional discontinuities) in the solar wind plasma (Neugebauer, 1985), with these current sheets having normals that are essentially perpendicular to the local magnetic field (Knetter et al., 2004). The velocity shear across the current sheets can be greater than the Alfvén speed and can approach the magnetosonic speed (Borovsky, 2012a), hence the shears can have magnetosonic Mach numbers ~1. Borovsky (2020a) has argued that the Alfvénic fluctuations look like a non-evolving heliospheric magnetic structure propagating outward at $0.7v_A$.

If the $\underline{k}$ vector of the Alfvénic fluctuation is purely perpendicular to $\underline{B}$, then the fluctuation has no group velocity: in that case, is the Alfvénic fluctuation an Alfvén wave? A longstanding question is whether these Alfvénic current sheets (Elsasser sheets) are rotational discontinuities propagating through the plasma or tangential discontinuities (plasma boundaries). Burkholder et al. (2019) point out that the Alfvénic signatures on the two sides of a discontinuity have their origins at different times from different locations in the corona. The outward-Alfvénic correlations in the solar wind statistically decay with distance from the Sun: it is an issue whether the decay is

caused by the destruction of the outward Alfvénic fluctuations or by the addition of inward Alfvénic fluctuations (Bruno and Bavassano, 1991).

Understanding the outward-traveling Alfvén waves is important for a number of reasons: (1) they may be integral to the acceleration of the solar wind, (2) they may power the turbulence in the solar wind which alters the evolution of the solar wind, (3) they affect the propagation and scattering of energetic particles throughout the inner heliosphere, and (4) their magnetic-field-direction fluctuations produce intermittent intervals of on-off driving of the Earth's magnetosphere by intermittently altering the dayside reconnection rate (an 'on' interval can produce a magnetospheric substorm).

A number of sources for the Alfvénic fluctuations in the solar wind have been considered. Because of the dominance of outward propagation, it is likely that a major source is at the Sun. The magnetic flux of the coronal-hole solar wind connects to the Sun via open-flux funnels that are caught in the downflow lanes at the edges of supergranules (Dowdy et al., 1987). Only a small fraction of the photospheric flux connects to the corona above. Most of the flux resides in low-lying loops that close before reaching coronal heights and temperatures. Photospheric motion jiggling the base of the open-flux funnels is one source of Alfvén waves, however the motion of the funnel in the downflow lane is probably more restrictive than the Leighton random walk in two dimensions. Jiggling of the closed chromospheric magnetic carpet and leakage of wavemodes from the chromosphere into the open funnels has also been considered (Cranmer and Ballegooijen, 2005). Reconnection of low-lying loops with the open-flux funnels (one possible source of plasma to the funnels) also will produce outward-Alfvénic perturbations (Fisk et al., 1999; Tu et al., 2005; Burkholder and Otto, 2019). Similarly, near the edges of coronal holes, reconnection of the open flux with the magnetic canopy of the corona will produce Alfvén waves. Another possibility is that turbulence near the Sun decays into a dynamic-alignment state, leaving one-side Alfvén waves (Dobrowolny et al., 1980; Matthaeus et al., 1983; Telloni et al., 2016).

Away from the Sun, the driving of inward and outward Alfvén waves by instabilities at velocity shears has been considered, in particular at CIR stream interfaces (Smith et al., 2011) and at the edges of coronal-plasma microstreams (Goldstein et al., 2003). Parametric instabilities have been invoked to create lower-frequency Alfvén waves in the solar wind from solar-origin higher-frequency Alfvén waves, and to create inward-propagating Alfvén waves (Bruno and Carbone,

2016). Higher-frequency Alfvén waves can be driven by various kinetic instabilities in the proton-alpha-electron solar-wind plasma. (Gary, 1993).

Excellent reviews of the origin of the Alfvénic fluctuations can be found (e.g. Velli and Pruneti, 1997; Cranmer and van Ballegooijen, 2005; Marsch, 2018). The near-Sun observations of Parker Solar Probe will provide valuable observations of a less-evolved Alfvén-wave spectrum from the Sun (e.g. Bale et al., 2019) and perhaps direct clues to the mechanisms producing the Alfvénic fluctuations. Future progress on this question will be helped by higher-resolution observations and simulations of open-flux funnels interacting with low and high closed loops, with simulations taking account of the granular and supergranular convection of closed flux.

2.7. Question 7: *How is solar-wind turbulence driven, what are its dynamics, and how is it dissipated?*

Active turbulence produces an energy transfer from large-scale fluctuations, into smaller-scale fluctuations, and then into the particle distribution functions in the form of heating. Fourier (advected) timescales of seconds to about an hour are believed to represent the spatial scales of active MHD turbulence in the solar wind. (Note however that the Fourier power in those frequencies comes dominantly from strong small-scale current sheets (directional discontinuities) in the solar wind plasma (Siscoe et al., 1968; Borovsky, 2010); and since the correlation function is the Fourier transform of the power spectral density, correlation functions are also expected to be dominated by the small-scale current sheets.) To understand the turbulence of the solar wind and its impact on the heliosphere, its driving, dynamics, and dissipation must be understood. How the turbulence is driven affects the evolution of the solar wind; how the turbulence is dissipated affects the evolution of the solar-wind particle distribution functions; the dynamical nature of the turbulent fluctuations affects the scattering and transport of energetic particles in the heliosphere.

Ideas about the driving of the turbulence involve extracting energy from outward propagating Alfvén waves (Goldstein et al., 1995) or from large-scale or mesoscale velocity shears (Roberts et al., 1987). It is well known that to produce a turbulent cascade of Alfvénic fluctuations to smaller spatial scales, counter propagating Alfvénic fluctuations are needed (Kraichnan, 1965): to tap the energy of outward-propagating Alfvén waves, inward-propagating Alfvén waves must first be created. Ideas to produce inward Alfvén waves include (a) the reflection of outward waves

975 (Verdini et al., 2009; Chandran and Hollweg, 2009), (b) parametric-decay instabilities (Tu et al.,
976 1989), and (c) the production of both inward and outward Alfvén waves at velocity shears (Breech
977 et al., 2008). Prominent solar wind shears include corotating interaction regions and the edges of
978 microstreams. Recent observations of optical flows in white light images (i.e. measuring the
979 motion of density features as a function of time) between 5 and 15 solar radii suggest that the solar
980 wind may begin in a highly filamentary state, with an abundance of mesoscale flow shears (De
981 Forest et al. 2018).

982 In the MHD range of spatial scales, the study of the dynamics of the turbulence focuses on
983 the nature of the fluctuations, the nature of the interactions between fluctuations, and on the physics
984 of the energy transfer to smaller scales. Major models of the MHD dynamics of the magnetic-field
985 and velocity fluctuations include the Maltese cross (Matthaeus et al., 1990), critical balance
986 (Goldreich and Sridhar, 1997), and scale-dependent dynamic alignment (Boldyrev, 2006), each
987 with different distributions of amplitude and spectral anisotropy of the fluctuations as functions of
988 scale size. Issues about the nonlinear interactions between fluctuations include selective decay
989 versus dynamic alignment, which evolve the turbulence toward different final states (Dobrowolny
990 et al., 1980; Matthaeus et al., 2008; Telloni et al., 2016). Compressibility of the turbulence is
991 another dynamic issue, as is the origin and role of pressure-balance structures in the solar wind
992 plasma. In the spatial-scales smaller than the MHD regime, the nature of the kinetic fluctuations
993 (e.g. whistler versus kinetic Alfvén wave versus inertial kinetic Alfvén wave) is not fully
994 understood (Gary and Smith, 2009; Carbone, 2012). The dynamics of the turbulence in the faster,
995 highly Alfvénic, quasi-homogeneous coronal-hole-origin solar wind is probably different from the
996 dynamics in slower, weakly Alfvénic or non-Alfvénic, inhomogeneous non-coronal-hole wind (Tu
997 et al., 2016). One universal consequence of the dynamics of active turbulence is “mixing”: an
998 attempt to quantify the amount of mixing occurring in the solar wind plasma between 0.3 and 1
999 AU found none (Borovsky, 2012b).

1000 In going from MHD spatial scales to kinetic spatial scales there is a breakpoint in the
1001 Fourier power spectrum of solar wind fluctuations, with the Fourier power being substantially
1002 reduced on the kinetic side of the spectral break. This breakpoint is taken as evidence of energy
1003 dissipation or mode conversion of MHD fluctuations at kinetic scales (Goldstein et al., 2015). At
1004 these kinetic spatial scales, investigators have focused on Landau damping and mode conversion

of Alfvén and kinetic-Alfvén waves with quasi-perpendicular wavevectors (Leamon et al., 1999), on ion-cyclotron damping and mode conversion of Alfvén waves with quasi-parallel wavevectors (Gary and Borovsky, 2004), on mode conversion of kinetic Alfvén waves (Podesta, 2012), and on magnetic-field reconnection across thin current sheets (Loureiro and Boldyrev, 2017). On the dissipation of the turbulence, the parametric instability of Alfvén waves can produce dissipation at all spatial scales (Shi et al., 2017). A data-analysis argument has been made that the physics of what determines the location of the spectral breakpoint is the physics of what determines the thicknesses of strong current sheets (directional discontinuities) in the solar wind plasma (Borovsky and Podesta, 2015); another argument has been made that the properties of the power spectrum above the breakpoint is owed to processes acting within the current sheets (Borovsky and Burkholder, 2020).

Relevant to this outstanding question, there are many excellent brief review articles (Goldstein et al., 1995, 2015; Horbury et al., 2005; Podesta, 2010; Matthaeus and Velli, 2011; Carbone, 2012; Oughton et al., 2015; Howes, 2015) and extensive review articles (e.g. Tu and Marsch, 1995; Schekochihin et al., 2009; Bruno and Carbone, 2013, 2016).

For future progress in understanding the nature of the MHD turbulence, the kinetic-scale fluctuations, the physics of current sheets, and the physics of dissipation, high-time-resolution very accurate multi-point measurements of the solar wind are badly needed (cf. Podesta, 2015; Vaivads et al. 2016; Cara et al., 2017; Howes, 2017; De Keyser et al., 2018), including separate measures of the ion velocities and the electron velocities.

2.8. Question 8: *How do the kinetic distribution functions of the solar wind evolve?*

The solar wind plasma is comprised of multiple particle populations: protons, an antisunward proton beam, an antisunward alpha-particle beam, core (cool) electrons, halo (hot) electrons, an antisunward electron strahl, and small numbers of highly ionized heavy ions. As the solar wind moves outward from the Sun, the particle populations evolve: the protons and alphas increase in temperature and specific entropy (Gary et al., 2000; Hellinger et al., 2011), the strahl intensity decreases (Maksimovic et al., 2005), the halo intensity increases (Maksimovic et al., 2005), and the proton and alpha beam speeds decrease (Marsch et al., 1982).

Note that the various particle distributions do not travel together: the proton distribution moves outward from the Sun at the "solar wind speed", the alpha particles and heavy ions stream through the protons moving outward along the local-magnetic-field direction at a fraction of the Alfvén speed faster than the protons, and electrons rapidly move along magnetic field lines Sunward and anti-Sunward at the individual electron speed. Driven by the free energy in beams and temperature anisotropies, there are multiple plasma-wave instabilities that couple the populations (Gary, 1993; Verscharen et al., 2015): the web of known interaction processes is sketched in Figure 8. The processes listed include weak double layers with antisunward-pointing electric fields that have been found in the solar wind plasma (*LaCombe et al.*, 2002): double layers can transfer energy and momentum between electrons and ions while most solar wind wave instabilities cannot.

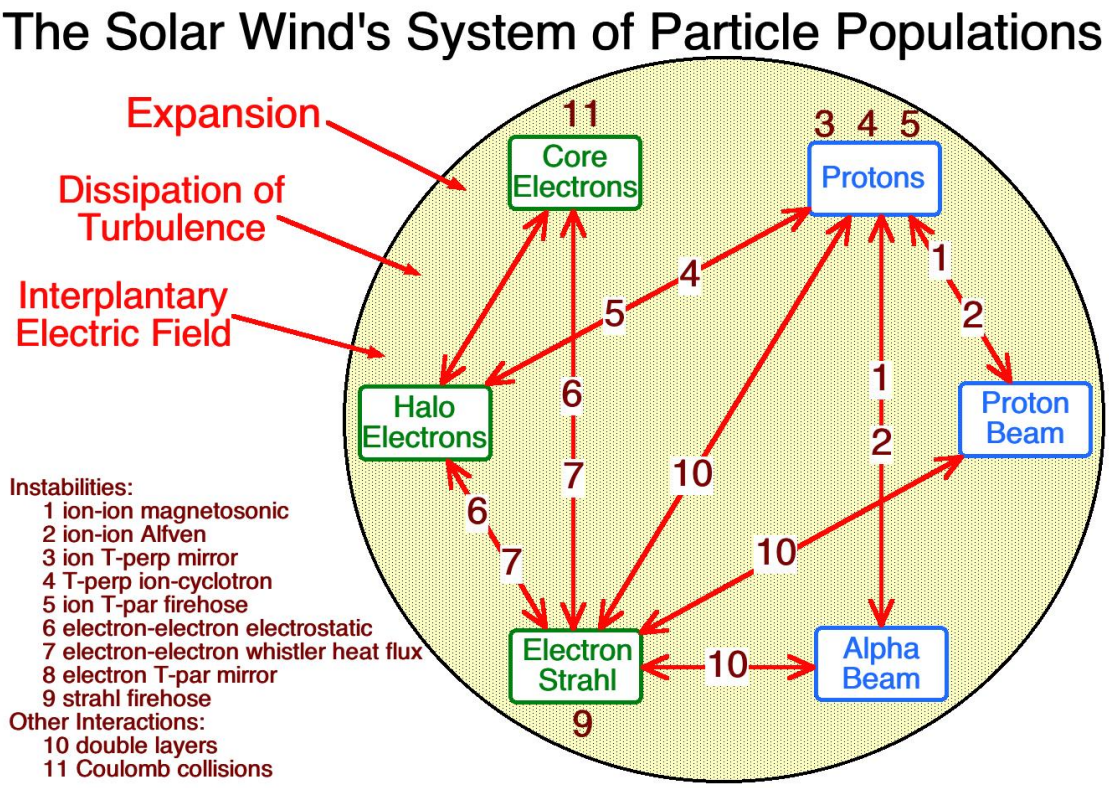

Figure 8. A systems science view of the solar wind comprised of distinct particle populations interacting via plasma instabilities. The black circle is the system, driven by (1) solar-wind expansion, (2) energy input from the dissipation of MHD turbulence, and (3) the interplanetary electric field. The green double arrows denote interactions between the populations (with special thanks to Peter Gary).

Understanding the nature and evolution of the multiple particle populations of the solar wind is important for several reasons: these populations carry the signatures of coronal and solar-wind physics, they drive the interplanetary electric field that contributes to solar wind acceleration, they affect the manner in which solar-wind turbulence is dissipated, they are the energy sink for that turbulence, and they are the carriers of solar wind heat flux and the determiners of where that power is deposited. The field-aligned strahl population is also important as a tracer of the local magnetic connectivity to the Sun (see Question 9) and as a probe of processes acting beyond the observing spacecraft.

The solar wind plasma can be thought of as a complex system wherein the various particle populations are the components (subsystems) of the system, with these components coupling to each other via plasma waves (cf. Figure 8): as is typical of a complex system, the natures of the couplings change as the subsystems co-evolve. A complex system (Lin et al., 2013) has multiple components, components that are not homogeneous, complicated interactions, and interactions that are nonlinear: the solar wind fits this definition. Adjectives describing the behavior of complex systems can be applied to a parcel of solar wind: driven (by expansion of the solar wind and by the dissipation of solar wind turbulence), dissipative (via Coulomb scattering), adaptive (by the evolution of the populations and their changing interactions), irreversible (because of Coulomb scattering), and open (energy is transferred to the plasma by the dissipation of turbulence and by electron heat flux from the Sun). A complex system also exhibits “emergence”: one emergent phenomenon in the solar wind may be the formation of a myriad of weak double layers to collectively produce the large-scale interplanetary potential (Lacombe et al., 2002; Salem et al., 2003; Lamy et al., 2003).

Excellent reviews of the kinetic evolution of the solar wind are available (Feldman and Marsch, 1997; Maksimovic et al., 2005; Marsch, 2006, 2018; Echim et al., 2011; Matteini et al. 2012; Pierrard et al., 2016; Matteini, 2016).

The velocity distribution functions of the particle populations at the Sun are not known: Parker Solar Probe’s measurements should provide key information about distributions at the Sun. Parker Solar Probe has exceptionally good instrumentation and the community looks forward to future data analysis efforts to further understand the physics of and evolution of the particle

populations of the solar wind. Beyond Parker Solar Probe, future progress in understanding the evolution of the particle populations in the heliosphere needs more-accurate and faster particle-distribution-function measurements (including heavy ions) correlated with high-quality plasma-wave measurements: such measurements may reveal active or past Landau resonances and active or past cyclotron resonances that are the fingerprints on the distribution functions of various wave-particle interactions.

2.9. Question 9: *What are the roles of solar wind structure and turbulence on the transport of energetic particles in the heliosphere?*

Steady progress is being made on the understanding and calculation of the transport of energetic particles through the solar wind, but it is still a major outstanding issue. Various particle populations are considered: electrons, protons, and heavy ions from solar flares and CME shocks, electrons and protons from CIR shocks, protons and electrons from Jupiter, cosmic rays from the outer heliosphere and beyond, and at lower energies, the electron strahl from the Sun.

Understanding the transport of energetic particles is important (1) for planning manned space exploration away from Earth, (2) for enabling energetic-particle measurements to be used for the understanding of the physics of particle acceleration, (3) for providing information about the structure of the heliosphere and its turbulence, and (4) for providing an understanding of particle transport in astrophysical plasmas.

To understand the transport of energetic particles in the heliosphere two things are needed. First, knowledge of the magnetic structure and magnetic connectedness of the heliosphere are needed (cf. Schatten, 1971; Kahler et al., 2016). Often this comes from heliospheric MHD simulations. Second, the scattering physics of particles in the heliospheric magnetic field needs to be understood. This might be as simple as obtaining perpendicular and parallel mean free paths to construct pitch-angle, parallel, and perpendicular diffusion coefficients to use in a diffusive transport equation (Zimbardo et al., 2012; Li, 2017). Increasingly sophisticated modeling is being used to estimate these values, including dynamic modeling with waves (Tautz and Shalchi, 2011; Gammon et al., 2019), and the modeling is producing increasingly better matches with observations.

On the issue of magnetic connectedness, there are some types of solar wind plasma that lack electron strahls: one such plasma type is the plasma associated with the sector-reversal region

around the heliospheric current sheet (Xu and Borovsky, 2015), also known as the very slow solar wind. This plasma originates as blobby impulsive emissions (a.k.a. puffs or plasmoids) from streamer-stalk regions (Suess et al., 2009; Foullon et al., 2011; Viall & Vourlidas, 2015). The magnetic field in this type of plasma is not Parker-spiral oriented and, as indicated by the absence of a strahl, it is unlikely that there is much contiguous magnetic flux that connects the Sun to this plasma in the heliosphere. Magnetic reconnection (Suess et al. 2009) at the top of the helmet streamer magnetic structure is the cause of the strahl dropouts (Kepko et al. 2016); counter-flowing plasma structures from the reconnection site are observed in the white light images around 5 solar radii (Sanchez-Diaz et al. 2017). The Earth is in this sector-reversal-region plasma about 20% of the time. When the Earth (or a measuring spacecraft) is in this type of plasma, solar energetic particle events (and lower-energy cosmic-ray fluxes) may be weaker than anticipated because of the lack of long-distance magnetic connections.

For the ducting of energetic particles in the heliosphere, the mesoscale structure of the solar wind magnetic field is very important. As discussed in Q5, the heliospheric field is largely structured into magnetic flux tubes separated by current sheets (Bruno et al., 2001); the magnetic tubes have narrow walls (current sheets, directional discontinuities) with large-angle changes in the magnetic-field direction across the walls with the interiors of the tubes having much lower levels of magnetic fluctuation. This produces an observed long-distance ducting of energetic particles (Bartley et al., 1966; McCracken et al., 1968; Gosling et al., 2004; Zimbardo, 2005; Trenchi et al., 2013; Kocharov et al., 2014; Borovsky, 2020b) consistent with the magnetic field lines being confined inside the tubes.

The flux-tube nature of the heliospheric magnetic field can also impact the physics of particle scattering (Michel, 1967; Qin and Li, 2008), with less scattering in the lower levels of fluctuations within the tubes. However, particles with finite gyroradii passing close to the tube walls will suffer large-angle scattering. In Table 4 some typical scale sizes of the solar-wind magnetic structure at 1 AU are listed: current sheets (tube walls), tube diameters, and the integral scale of the magnetic power spectral density. At 1 AU (taking B = 5 nT) current sheets are about as thick as the gyroradius of an 11-keV proton. Hence, protons with energies above ~11 keV (or electrons above ~4 MeV) could suffer sudden strong (~90^o) changes in their pitch angles in less than a gyroperiod. At 1 AU, flux tubes have diameters on the order of the gyroradius of 210-MeV

protons. Protons with energies well below 210 MeV can be ducted in the relatively quiet tubes; for protons with energies much greater than ~210 MeV the tubes would act as scatterers, since adjacent tubes can have magnetic-field orientations that significantly differ. Using pitch-angle-diffusion coefficients based on the amplitude of a Power spectra and the assumption of random phases in the spectra may not capture the strong scattering of the intermittent structures (walls) and the long mean-free-paths of the tube interiors. Additionally, the flux tubes at 1 AU have local curvatures with wandering wavelengths that are on the order of 0.07 AU along the Parker-spiral direction (Tong et al., 2016), which may play a role in the scattering of very energetic particles (e.g. Webb et al., 2006).

Excellent reviews of the transport of energetic particles in the solar wind can be found (e.g. Cliver, 2001; Giacalone and Jokipii, 2001; Richardson, 2004; Zimbardo et al., 2012; Reames, 2013; Malandraki, 2015; Cohen, 2016; Li, 2017), as well as explorations of the effects of intermittency on the transport (Michel, 1967; Fisk and Sari, 1973; Borovsky, 2008; Qin and Li, 2008; Trenchi et al., 2013; Pucci et al., 2016; Droge et al., 2018).

For future progress on this question, more multipoint observations are crucial. The in situ measurements of Parker Solar Probe and Solar Orbiter near the Sun combined with energetic-particle measurements at STEREO and at Earth will be particularly valuable. Exploration of the properties of the electron strahl to reveal the properties of the structure and connectivity of the heliospheric magnetic field could be fruitful. Advancing our understanding of the nature and dynamics of the mesoscale structure of the solar wind plasma via faster and more-accurate in situ measurements combined with more-advanced plasma simulations will also be productive.

Table 4. The scale size of typical magnetic structures in the solar wind at 1 AU and the energies of particles with an equivalent gyroradius assuming B = 5 nT.

	Advection Timescale	Thickness	Proton Energy	Electron Energy	Proton Gyroperiod	Electron Gyroperiod
Current Sheet	6 sec	3000 km	11 keV	4 MeV	13 sec	0.063 sec
Flux Tube	15 min	4.4×10^5 km	210 MeV	660 MeV	16 sec	9.2 sec
Outer Scale	2 hr	3.6×10^6 km	4.5 GeV	5.8 GeV	77 sec	75 sec

3. Discussion: Other Important Questions

To develop the list of nine solar wind questions (Table 1), dozens of heliospheric researchers were polled. From the contributed lists of questions from many heliospheric scientists, a few that were repeatedly mentioned were not discussed in this commentary. One dealt with CME creation, evolution, and impact on the global structure of the heliosphere (see Burkepile et al., 2004; Gopalswamy (2016); Kilpua et al. 2017; 2019 and Thompson et al. 2020 for reviews of the research and outstanding questions). A second dealt with the interaction of the solar wind with the interstellar medium: excellent reviews on that topic can be found (Burlaga, 2015; Zank, 2015; Burlaga et al., 2018). Other topics less extensively mentioned were about shock physics, seed-particle populations, dust, and pickup ions.

Finally, an important question related to space weather and the Sun-Earth connection is where to locate a single solar wind monitor or a network of monitors for the Earth (Sandahl et al., 1996; Biesecker et al., 2007; Ashour-Abdalla et al., 2008). The activity and evolution of the Earth's magnetosphere is driven (a) chiefly by magnetic-field reconnection with the shocked solar wind plasma on the dayside edge of the magnetosphere (Dungey, 1961) and (b) to a minor extent by a "viscous interaction" with the solar wind (Axford and Hines, 1961), the physics of the latter being little understood. In the dayside-reconnection driving, it is not the energy release of reconnection that does the driving, rather it is the fact that dayside reconnection magnetically connects the magnetosphere to the moving solar wind. The rate of dayside reconnection, which largely controls the rate of driving, depends on the orientation of the solar wind magnetic field, and on the speed, density, magnetic-field strength, and Mach number of the solar wind (Borovsky and Birn, 2014). The reconnection rate is very sensitive to the clock angle of the solar wind magnetic-field vector as seen from Earth (Komar et al., 2015), on timescales of less than 1 minute.

The standard practice has been to put a solar wind monitor in orbit around the L1 point, 230 $R_E \approx 0.01$ AU upstream of the Earth (King and Papitashvili, 2005; Weimer and King, 2008). A problem with this is that the solar wind that hits the monitor is not the solar wind that hits the Earth: owing to the high variability of the direction of the solar wind flow vector and to aberration

of the solar wind flow by the Earth's orbital motion about the Sun, an L1 monitor is rarely on a flow streamline that connects to the Earth (Borovsky, 2018; Walsh et al., 2019). Correlation scales of the solar-wind magnetic-field direction transverse to its flow are on the order of 50 R_E (Zastenker et al., 2000; Richardson and Paularena, 2001) and the L1 monitor's streamline can easily miss the Earth by that amount. The space weather community and a large part of the magnetospheric research community both rely on accurate solar wind information and improvements over single monitors located at L1 are needed. One solution that preserves some space-weather warning time is a swarm of monitors about the L1 point; one solution that yields more accuracy as to what is hitting the magnetosphere is a set of monitors in ~30 R_E circular orbits about the Earth, similar to the NASA IMP (Interplanetary Monitoring Platform) constellation of the 1970's (Feldman et al., 1978; Butler, 1980). Alternatives to an L1 monitor are spacecraft with imaging suites located over the poles of the Sun, or at L5 (Gibney 2017; Thomas et al. 2018).

4. Outlook -- What are the needs and prospects for future progress?

In discussing the individual outstanding questions in Section 2, specific needs for the future were called out. There are common themes to these needs.

Certainly, solar wind physics needs accurate solar models and accurate solar wind propagation models that can resolve mesoscale structures. At the Sun, fully 3-dimensional, time-dependent models of solar wind sources and acceleration are needed. The time dependence must at the least include the differential rotation of the photosphere, supergranulation, and the evolving magnetic field. Away from the Sun, reliable modeling of quiescent background solar wind is needed. The solar wind plasma and the heliospheric magnetic field, with compressions, rarefactions, and fluctuations, are the ground state of space weather. The quiescent solar wind preconditions the magnetosphere before major storms and that preconditioning changes the manner in which the magnetosphere reacts during the storm. The quiescent solar wind is the medium through which CMEs propagate, and from which CIRs form. The quiescent solar wind is also the medium through which solar energetic particles are transported. Future modeling needs to go beyond the large-scale no-detail fast-versus-slow level to capture mesoscale structure, microstreams, and fluctuation amplitudes. Another need for future progress is advancements in plasma physics pertaining to the weakly collisional solar wind: treatments of collisionless viscosity, non-Maxwellian thermodynamics, heating without collisions, and the origin of suprathermal populations.

Solar observations needed for future progress include regular backside magnetograms and polar magnetograms. The location of the heliospheric current sheet, and the region on the Sun that Earth or a spacecraft is connected to is not well determined, largely as a result of the lack of information on the polar magnetic field and time-evolving magnetic field on the backside that we currently do not observe. EUV imagers are limited to the low corona, while white light imagers are currently limited to the outer corona and heliosphere, due to the need to block out the bright photosphere below, and the scattered light associated with that. Natural solar eclipses are exceptions to this requirement, but provide little time coverage. The region in between these two instrumental regimes is sometimes called the ‘middle corona’, and spans the region up to a few

solar radii. This is the region in which many of the processes described in Q1, Q2, and Q3 occur, and it is the region where the magnetic fields and connectivity are highly non-radial. Continuous measurements of temperature, flow velocity, and magnetic field in the middle corona would provide the link from the low corona to the solar wind. Spectroscopy on disk, and off disk, especially with sulfur and elements of different FIP, will be important for direct relation with in situ tracers.

Parker Solar Probe is yielding (e.g. Versharen, 2019; Parker 2019), and DKIST and Solar Orbiter are going to yield, unprecedented high-quality plasma and field measurements close to the Sun, revealing some of the plasma physics of the transition from corona to solar wind. Solar Orbiter will get some backside magnetograms and a polar view of the magnetic field. The solar wind measurements most needed for the future will be high-time-resolution high-accuracy multipoint measurements of the plasma, flow, magnetic field, and ion composition to discern the nature and physics of the solar wind's ubiquitous fluctuations.

Acknowledgements. To initiate this commentary, dozens of scientists in the solar wind research community were individually asked to create a list of what they thought were the outstanding questions in solar wind physics. We chose to comment on nine questions from the full list of suggestions. The authors thank Nick Arge, Doug Biesecker, Joan Burkepile, Ben Chandran, Ed Cliver, Christina Cohen, Georgia de Nolfo, Craig DeForest, Mihir Desai, Bill Feldman, Peter Gary, Joe Giacalone, Nat Gopalswamy, Aleida Higginson, Tim Horbury, Bernie Jackson, Steve Kahler, Harald Kucharek, Jon Linker, Janet Luhmann, Benjamin Lynch, Peter MacNeice, Bob McPherron, John Podesta, Ian Richardson, Aaron Roberts, Nathan Schwadron, Chuck Smith, Angelos Vourlidas, Peter Young, Samantha Wallace, Rob Wicks, and Dan Weimer for their help. JB was supported by the NSF SHINE program via award AGS-1723416, by the NASA Heliophysics Guest Investigator Program via grant NNX17AB71G, by the NASA Heliophysics LWS program via grants NNX16AB75G, NNX14AN90G, and by the NSF GEM Program. NMV is supported by the NASA Heliophysics Internal Scientist Funding Model. No data were used in the preparation of this manuscript.

The authors thank the two reviewers, Susan Lepri and Marco Velli, for their thoughtful and constructive comments on this manuscript.

References

Adams, W. M. (1976). Differential rotation of photospheric magnetic fields associated with coronal holes, *Solar Physics, 47,* 601, 1976.

Antiochos, S. K., Linker, J. A., Lionello, R., Mikic, Z., Titov, V., and Zurbuchen, T. H. (2012). The structure and dynamics of the corona-heliosphere connection. *Space Science Reviews, 172*, 169.

Arge, C. N., Luhmann, J. G., Odstrcil, D., Schrijver, C. J., & Li, Y. (2004). Stream structure and coronal sources of the solar wind during the May 12th, 1997 CME. *Journal of Atmospheric and Solar-Terrestrial Physics, 66*, 1295

Arge, C. N., Henney, C. J., Gonzalez hernandez, I., Toussaint, W. A., Koller, J., & Godinez, H. C. (2013). Modeling the corona and solar wind using ADAPT maps that include far-side observations. *AIP Conference Proceedings, 1539*, 11

Arya, S., & Freeman, J. W. (1991). Estimates of solar wind velocity gradients between 0.3 and 1 AU based on velocity probability distributions from Helios 1 at perihelion and aphelion. *Journal of Geophysical Research, 96*, 14183, 1991.

Asbridge, J. R., Bame, S. J., Feldman, W. C., & Montgomery, M. D. (1976). Helium and hydrogen velocity differences in the solar wind. *Journal of Geophysical Research, 81,* 2719.

Ashour-Abdalla, M., Walker, R. J., Peroomian, V., & El-Alaoui, M. (2008). On the importance of accurate solar wind measurements for studying magnetospheric dynamics. *Journal of Geophysical Research, 113*, A08204.

Axford, W. I., & Hines, C. O. (1961). A unifying theory of high-latitude geophysical phenomena and geomagnetic storms, *Canadian Journal of Physics, 39*, 1433.

Bale, S. D., Badman, S. T., Bonnell, J. W., Bowen, T. A., Burges, D., et al. (2019) Highly structured slow solar wind emerging from an equatorial coronal hole. *Nature, 576*. 237

Baker, D., van Driel-Gesztelyi, L., & Attril, G. R. R. (2007). Evidence for interchange reconnection between a coronal hole and an adjacent emerging flux region. *Astronomische Nachrichten, 328*, 773.

Bame, S. J., Asbridge, J. R., Feldman, W. C., & Gosling, J. T. (1976). Solar cycle evolution of high-speed solar wind streams. *The Astrophysical Journal, 207*, 977.

Bartley, W. C., Bakata, R. P., McCracken, K. G., & Rao, U. R. (1966). Anisotropic cosmic radiation fluxes of solar origin. *Journal of Geophysical Research, 71,* 3297.

Belcher, J. W., & Davis, L. (1971) Large amplitude Alfvén waves in the interplanetary medium, 2. *Journal of Geophysical Research, 76*, 3534.

Bemporad, A. (2017). Exploring the inner acceleration region of solar wind: A study based on coronagraphic UV and visible light data. *The Astrophysical Journal, 846,* 86

Biesecker, D. A., Webb, D. F., & St. Cyr, O. C. (2007). STEREO space weather and the Space Weather Beacon. *Space Science Reviews, 136*, 45

Boldyrev, S., Spectrum of magnetohydrodynamic turbulence, *Physical Review Letters, 96*, 115002, 2006.

Boldyrev, S., JPerez, J. C., Borovsky, J. E., & Podesta, J. J. (2011). Spectral scaling laws in magnetohydrodynamic turbulence simulations and in the solar wind. *The Astrophysical Journal Letters, 741,* L19.

Borovsky, J. E. (2006). Eddy viscosity and flow properties of the solar wind: Co-rotating interaction regions, coronal-mass-ejection sheaths, and solar-wind/magnetosphere coupling, *Physics of Plasmas, 13,* 056505.

Borovsky, J. E. (2008). The flux-tube texture of the solar wind: Strands of the magnetic carpet at 1 AU? *Journal of Geophysical Research, 113,* A08110.
Borovsky, J. E. (2010). On the contribution of strong discontinuities to the power spectrum of the solar wind. *Physical Review Letters*, 105, 111102.
Borovsky, J. E. (2012a). The effect of sudden wind shear on the Earth's magnetosphere: Statistics of wind-shear events and CCMC simulations of magnetotail disconnections. *Journal of Geophysical Research, 117*, A06224.
Borovsky, J. E. (2012b). Looking for evidence of mixing in the solar wind from 0.31 to 0.98 AU. *Journal of Geophysical Research, 117,* A06107.
Borovsky, J. E. (2012c). The velocity and magnetic-field fluctuations of the solar wind at 1 AU: Statistical analysis of Fourier spectra and correlations with plasma properties. *Journal of Geophysical Research, 117*, A05104.Borovsky, J. E. (2016). Plasma structure of the coronal-hole solar wind: Origins and Evolution. *Journal of Geophysical Research, 121*, 5055.
Borovsky, J. E. (2018). The spatial structure of the oncoming solar wind at Earth. *Journal of Atmospheric and Solar-Terrestrial Physics, 177*, 2.
Borovsky, J. E. (2020a). On the motion of the heliospheric magnetic structure through the solar wind plasma. *Journal of Geophysical Research*, 2019JA027377, in press
Borovsky, J. E. (2020b). The magnetic structure of the solar wind: Ionic composition and the electron strahl. *Geophysical Research Letters*, 2019GL084586, in press
Borovsky, J. E. (2020c) What magnetospheric and ionospheric researchers should know about the solar wind. submitted to *Journal of Atmospheric and Solar-Terrestrial Physics*, JASTP-D-19-00125
Borovsky, J. E., & Birn, J. (2014). The solar-wind electric field does not control the dayside reconnection rate. *Journal of Geophysical Research, 119*, 751.
Borovsky, J. E., & Burkholder, B. L. (2020). On the Fourier contribution of strong current sheets to the high-frequency magnetic power spectral density of the solar wind. *Journal of Geophysical Research*, 2019JA027307, in press
Borovsky, J. E., & Denton, M. H. (2010). Solar-wind turbulence and shear: A superposed-epoch analysis of corotating interaction regions at 1 AU. *Journal of Geophysical Research*, 115, A10101.
Borovsky, J. E., & Denton, M. H. (2016a). The trailing edges of high-speed streams at 1 AU. *Journal of Geophysical Research, 121*, 6107.
Borovsky, J. E., & Denton, M. H. (2016b). Compressional perturbations of the dayside magnetosphere during high-speed-stream-driven geomagnetic storms. *Journal of Geophysical Research, 121*, 4569.
Borovsky, J. E., & Gary, S. P. (2009). On viscosity and the Reynolds number of MHD turbulence in collisionless plasmas: Coulomb collisions, Landau damping, and Bohm diffusion. *Physics of Plasmas, 16*, 082307.
Borovsky, J. E., & Gary, S. P. (2014). How important are the alpha-proton relative drift and the electron heat flux for the proton heating of the solar wind in the inner heliosphere? *Journal of Geophysical Research, 119*, 5210.
Borovsky, J. E., & Podesta, J. J. (2015). Exploring the effect of current-sheet thickness on the high-frequency Fourier spectrum of the solar wind. *Journal of Geophysical Research, 120*, 9256.
Borovsky, J. E., Birn, J., Echim, M. M., Fujita, S., Lysak, R. L., Knudsen, D. J., Marghitu, O., Otto, A., Watanabe, T.-H., & Tanaka, T. (2019). Quiescent discrete auroral arcs: A review of

magnetospheric generator mechanisms. submitted to *Space Science Reviews*, SPAC-D-19-00040.
Breech, B., Matthaeus, W. H., Minnie, J., Bieber, J. W., Oughton, S., Smith, C. W., and Isenberg, P. A. (2008). Turbulence transport throughout the heliosphere. *Journal of Geophysical Research, 113*, A08105.
Bruno, R. (2019). Intermittency in solar wind turbulence from fluid to kinetic scales. *Earth and Space Science, 6,* 656
Bruno, R., & Bavassano, (1991). Origin of low cross-helicity regions in the inner solar wind. *Journal of Geophysical Research, 96*, 7841.
Bruno, R., & Carbone, V. (2013). The solar wind as a turbulence laboratory, *Living Reviews of Solar Physics, 10*, 2, http://www.livingreview.org/lrsp-2013-2.
Bruno, R., & Carbone, V. (2016). Turbulence in the solar wind. *Lecture Notes in Physics, 928*, 1.
Bruno, R., Bavassano, B., Bianchini, L., Pietropaolo, E., Villante, U., Carbone, V., & Veltri, P. (1999). Solar wind intermittency studied via local intermittency measure. *ESA Special Publications, 448*, 1147
Bruno, R., Carbone, V., Veltri, P., Pietropaolo, E., & Bavassano, B. (2001). Identifying intermittency events in the solar wind. *Planetary and Space Science, 49*, 1201.
Burkepile, J. T., Hundhausen, A. J., Stranger, A. L., St. Cyr, O. C., & Seiden, J. A. (2004). Role of projection effects on solar coronal mass ejection properties: 1. A study of CMEs associated with limb activity. *Journal of Geophysical Research, 109*, A03103
Burkholder, B. L. & Otto, A. (2019). Magnetic reconnection of solar flux tubes and coronal reconnection signatures in the solar wind at 1 AU. submitted to *Journal of Geophysical Research*, 2019JA027114.
Burkholder, B., Otto, A., Delamere, P., & Borovsky, J. E. (2019). Magnetic connectivity in the corona as a source of structure in the solar wind. *Journal of Geophysical Research, 124*, 32.
Burlaga, L. (2015). Voyager observations of the magnetic field in the heliosheath and the local interstellar medium. *Journal of Physics: Conference Series, 642*, 012003.
Burlaga, L. F.; Forman, Miriam A. (2002) Large-scale speed fluctuations at 1 AU on scales from 1 hour to ≈1 year: 1999 and 1995, Journal of Geophysical Research (Space Physics), 107, Issue A11, CiteID 1403, DOI 10.1029/2002JA009271.
Burlaga, L. F., Florinkski, V., & Ness, N. F. (2018). Turbulence in the outer heliosheath. *The Astrophysical Journal, 854*, 20.
Butler, P. (1980). Interplanetary Monitoring Program engineering history and achievement. NASA TM-80758. NASA Goddard Space Flight Center, Greenbelt, Maryland
Cahill, L. J., Jr.; Winckler, J. R. (1992) Periodic magnetopause oscillations observed with the GOES satellites on March 24, 1991, Journal of Geophysical Research, 97, 8239
Camporeale, E., Care, A., & and Borovsky, J. E. (2017). Classification of solar wind with machine learning. *Journal of Geophysical Research, 122*, 10910
Caplan, R. M., Downs, C., & Linker, J. A. (2016). Synchronic coronal hole mapping using multi-instrument EUV images: Data preparation and detection method. *The Astrophysical Journal, 823*, 53
Cara, A., Lavraud, B., Fedorov, A., De Keyser, J., DeMarco, R., Marcucci, M. F., Valentini, F., Servidio, S., & Bruno, R. (2017). Electrostatic analyzer design for solar wind proton measurements with high temporal, energy, and angular resolutions. *Journal of Geophysical Research, 122*, 1439.

Carbone, V. (2012). Scalings, cascade and intermittency in solar wind turbulence. *Space Science Reviews, 172*, 343.
Chandran, B. D. G., & Hollweg, J. V. (2009). Alfven wave reflection and turbulent heating in the solar wind from 1 solar radius to 1 AU: An analytical treatment. *The Astrophysical Journal, 707*, 1659
Cirtain, J. W.; Golub, L.; Lundquist, L.; van Ballegooijen, A.; Savcheva, A.; Shimojo, M.; DeLuca, E.; Tsuneta, S.; Sakao, T.; Reeves, K.; Weber, M.; Kano, R.; Narukage, N.; Shibasaki, K. (2007) Evidence for Alfvén Waves in Solar X-ray Jets, Science, 318, 1580
Claudepierre, S. G.; Hudson, M. K.; Lotko, W.; Lyon, J. G.; Denton, R. E. (2010) Solar wind driving of magnetospheric ULF waves: Field line resonances driven by dynamic pressure fluctuations, Journal of Geophysical Research: Space Physics, Volume 115, Issue A11, CiteID A11202
Cliver, E. W. (2001) Solar energetic particles: Acceleration and transport. *AIP Conference Proceedings, 516*, 103
Close, R. M.; Parnell, C. E.; Longcope, D. W.; Priest, E. R. (2004) Recycling of the Solar Corona's Magnetic Field, The Astrophysical Journal, 612, 81
Close, R. M., Parnell, C. E., Longcope, D. W., & Priest, E. R. (2005). Coronal flux recycling times. *Solar Physics, 231*, 45.
Cohen, C. M. S. (2016). Current understanding of SEP acceleration and transport. *AIP Conference Proceedings, 1720*, 060001.
Coleman, P. J. (1968). Turbulence, viscosity, and dissipation in the solar-wind plasma. *The Astrophysical Journal, 153*, 371.
Cranmer, S. R. (2009), Coronal Holes, Living Reviews in Solar Physics, 6, 3
Cranmer, S. R., van Ballegooijen, A. A., Edgar, R. J., (2007) Self-consistent Coronal Heating and Solar Wind Acceleration from Anisotropic Magnetohydrodynamic Turbulence, The Astrophysical Journal Supplement Series, 171, 520
Cranmer, S. R., & van Ballegooijen, A. A. (2005). On the generation, propagation, and reflection of Alfvén waves from the solar photosphere to the distant heliosphere. *The Astrophysical Journal Supplement Series, 156*, 265.
Cranmer, S. R., Gibson, S. E., & Riley, P. (2017). Origins of the ambient solar wind: Implications for space weather. *Space Science Reviews, 212*, 1345.
Crooker, N. U.; Gosling, J. T.; Kahler, S. W. (2002) Reducing heliospheric magnetic flux from coronal mass ejections without disconnection, Journal of Geophysical Research, 107, 1028, DOI 10.1029/2001JA000236
Crooker, N. U., Antiochos, S. K., Zhao, X., & Neugebauer, M. (2012). Global network of solar wind. *Journal of Geophysical Research, 117*, A04104.
Crooker, N. U., Burton, M. E., Siscoe, G. L., Kahler, S. W., Gosling, J. T., Smith, E. J. (1996) Solar wind streamer belt structure. *Journal of Geophysical Research, 101*, 24331
D'Amicis, R., & Bruno, R., (2015). On the origin of highly Alfvénic slow solar wind. *The Astrophysical Journal, 805*, 84.
D'Amicis, R., Matteini, L., & Bruno, R. (2019). On the slow solar wind with high Alfvénicity: from composition and microphysics to spectral properties. *Monthly Notices of the Royal Astronomical Society, 483*, 4665.
De Keyser, J., Lavraud, B., Prech, L., Neefs, E., Berkenbosch, S, Beeckman, B., Fedorov, A., Marcucci, M. F., De Marco, R., & Brienza, D. (2018). Beam tracking strategies for fast

acquisition of solar wind velocity distribution functions with high energy and angular resolutions. *Annales Geophysicae, 36,* 1285.

DeForest, C. E.; Matthaeus, W. H.; Viall, N. M.; Cranmer, S. R. (2016) Fading Coronal Structure and the Onset of Turbulence in the Young Solar Wind, The Astrophysical Journal, 828, 66

DeForest, C. E.; Howard, R. A.; Velli, M.; Viall, N.; Vourlidas, A. (2018) The Highly Structured Outer Solar Corona, The Astrophysical Journal, 862, 18

Del Zanna, G., Aulanier, G., Klein, K. –L., and Török, T., (2011) A single picture for solar coronal outflows and radio noise storms, Astronomy and Astrophysics, 526, A137

Del Zanna, G. & Mason, H.E. (2018) Solar UV and X-ray spectral diagnostics, *Living Rev Sol Phys 15*: 5. https://doi.org/10.1007/s41116-018-0015-3

De Pontieu, B.; McIntosh, S. W.; Carlsson, M.; Hansteen, V. H.; Tarbell, T. D.; Boerner, P.; Martinez-Sykora, J.; Schrijver, C. J.; Title, A. M. (2011) The Origins of Hot Plasma in the Solar Corona, Science, 331, 55

De Toma, G., and Arge, C. N., (2005) Multi--wavelength Observations of Coronal Holes, Large-scale Structures and their Role in Solar Activity ASP Conference Series, Vol. 346, Proceedings of the Conference held 18-22 October, 2004 in Sunspot, New Mexico, USA. Edited by K. Sankarasubramanian, M. Penn, and A. Pevtsov, p.251

Di Matteo S., Viall, N. M., Kepko L., Wallace, S., Arge, C. N., MacNeice P., (2019) Helios Observations of Quasiperiodic Density Structures in the Slow Solar Wind at 0.3, 0.4, and 0.6 AU, Journal of Geophysical Research, 124, 2, https://doi.org/10.1029/2018JA026182

Dobrowolny, M., Mangeney, A., & Veltri, P. (1980). Fully developed anisotropic turbulence in interplanetary space. *Physical Review Letters, 45*, 144.

Dowdy, J. F., Emslie, A. G., & Moore, R. L. (1987). On the inability of magnetically constricted transition regions to account for the 10^5 to 10^5 K plasma in the quiet solar atmosphere. *Solar Physics, 112*, 255.

Droge, W., Kartavykh, Y. Y., Wang, L., Telloni, D., & Bruno, R. (2018). Transport modeling of interplanetary electrons in the 2002 October 20 solar particle event. *The Astrophysical Journal, 869*, 168.

Durovcova, T., Nemecek, Z., & Safrankova, J. (2019). Evolution of the α-proton differential motion across steam interaction regions. *The Astrophysical Journal, 873*, 24.

Dungey, J. W. (1961). Interplanetary magnetic field and the auroral zones. *Physical Review Letters, 6*, 47.

Dyrud, L. P.; Behnke, R.; Kepko, E. L.; Sulzer, M.; Zafke, S. (2008) Ionospheric ULF oscillations driven from above Arecibo, Geophysical Research Letters, Volume 35, Issue 14, CiteID L14101

Echim, M. M., Lemaire, J., & Lie-Svendsen, O. (2011). A review on solar wind modeling: Kinetic and fluid aspects. *Surveys of Geophysics, 32*, 1.

Endeve, E., O. Lie‐Svendsen, V. H. Hansteen, and E. Leer (2005), Release of helium from closed‐field regions of the Sun, *Astrophys. J., 624*, 402–413, doi:10.1086/428938.

Feldman, U., & Widing, K. C. (2002). A review of the first ionization potential effects on elemental abundances in the solar corona and in flares. *Physics of Plasmas, 9*, 629

Feldman, U., Widing, K. G., & Warren, H. P. (1999). Morphology of the quiet solar upper atmosphere in the $4x10^4 < T_e < 1.4x10^6$ K temperature regime. *The Astrophysical Journal, 522*, 1133.

Feldman, U., Landi, E., & Schwadron, N. A. (2005). On the sources of fast and slow solar wind. *Journal of Geophysical Research, 110*, A07109.

Feldman, W. C., & Marsch, E. (1997). Kinetic Phenomena in the Solar Wind. in *Cosmic Winds and the Heliosphere*. J. R. Jokipii, C. P. Sonett, and M. S. Giampapa (eds), pg. 617-676, University of Arizona Press, Tucson.

Feldman, W. C., Asbridge, J. R., Bame, S. J., & Gosling, J. T. (1978). Long-term variations of selected solar wind properties: Imp 6, 7, and 8 results. *Journal of Geophysical Research, 83*, 2177

Feldman, W. C., Anderson, J., Bohlin, J. D., Bulaga, L. F., Farquhar, R., Gloeckler, G., Goldstein, B. E., Harvey, J. W., Holzer, T. E.,, Jones, W. V., Kellogg, P. J.,m Drimigis, S. M., Kundu, M. R., Lazarus, A. J., Mellott, M. M., Parker, E. N., Rosner, R., Rottman, G. J., Slavin, J. A., Suess, S. T., Tsurutani, B. T., Woo, R. T., & Zwickl, R. D. (1990). The Solar Probe mission. *AIP Conference Proceedings, 203*, 101.

Fenrich, F. R.; Waters, C. L. (2008) Phase coherence analysis of a field line resonance and solar wind oscillation, Geophysical Research Letters, Volume 35, Issue 20, CiteID L20102

Fisk, L. A., (2003) Acceleration of the solar wind as a result of the reconnection of open magnetic flux with coronal loops, Journal of Geophysical Research (Space Physics), 108, 1157, DOI 10.1029/2002JA009284

Fisk, L., & Sari, J. W. (1973). Correlation length for interplanetary magnetic field fluctuations. *Journal of Geophysical Research, 78*, 6729.

Fisk, L. A., Schwardron, N. H., & Zurbuchen, T. H., (1999). Acceleration of the fast solar wind by the emergence of new magnetic flux. Journal of Geophysical Research, 104, 19765.

Foullon, C., Lavraud, B., Luhmann, J. G., Farrugia, C. J., Retino, A., Simunac, K. D. C., Wardle, N. C., Galvin, A. B., Kucharek, H., Owen, C. J., Popecki, M., Otitz, A., & Sauvaud, J.-A. (2011). Plasmoid releases in the heliospheric current sheet and associated coronal hole boundary layer evolution. *The Astrophysical Journal, 737*, 1.

Fox, N. J., Velli, M. C., Bale, S. D., Decker, R., Driesman, A., Howard, R. A., Kasper, J. C., Kinnison, J.,m Kusterer, M., Lario, D., Lockwood, M. K., McComas, D. J., Raouafi, N. E., & Szabo, A. (2016). The solar Probe Plus mission: Humanity's first visit to our star. *Space Science Reviews, 204*, 7

Freeman, J. W. (1988). Estimates of solar wind heating inside 0.3 AU. *Geophysical Research Letters, 15*, 88.

Freeman, M. P., & Morley, S. K. (2009). No evidence for externally triggered substorms based on superposed epoch analysis of IMF Bz. *Geophysical Research Letters, 36*, L21101.

Gammon, M., Heusen, M., & Shalchi, A. (2019), Comparison between test-particle simulations and test-particle theories for cosmic ray transport: III. Dynamical turbulence. *Journal of Physics Communications, 3*, 015016.

Gary, S. P., (1993). *Theory of Space Plasma Microinstabilities*. Cambridge University Press, New York.

Gary, S. P., & Borovsky, J. E. (2004). Alfvén-cyclotron fluctuations: Linear Vlasov theory. *Journal of Geophysical Research, 109*, A06105.

Gary, S. P., & Smith, C. W. (2009). Short-wavelength turbulence in the solar wind: Linear theory of whistler and kinetic Alfvén fluctuations. *Journal of Geophysical Research, 114*, A12105.

Gary, S. P., Yin, L., Winske, D., & Reisenfeld, D. B. (2000). Electromagnetic alpha/proton instabilities in the solar wind. *Geophysical Research Letters, 27*, 1355.

Giacalone, J., & Jokipii, J. R. (2001). The transport of energetic particles and cosmic rays in the heliosphere. *Advances in Space Research, 27*(3), 461

Gloeckler, G., Zurbuchen, T. H., & Geiss, J. (2003). Implications of the observed anticorrelation between solar wind speed and coronal electron temperature. *Journal of Geophysical Research, 108*, 1158.

Goldreich, P., & Sridhar, S. (1997). Magnetohydrodynamic turbulence revisited. *The Astrophysical Journal, 485*, 680.

Goldstein, M. L., Roberts, D. A., & Matthaeus, W. H. (1995). Magnetohydrodynamic turbulence in the solar wind, *Annual Review of Astronomy and Astrophysics, 33*, 283.

Goldstein, M. L., Roberts, D. A., & Deane, A. (2003). The effect of microstreams on Alfvénic fluctuations in the solar wind. *AIP Conference Proceedings, 679*, 405.

Goldstein, M. L., Wicks, R. T., Perri, S., & Sahraoui, F. (2015). Kinetic scale turbulence and dissipation in the solar wind: key observational results and future outlook. *Philosophical Transactions of the Royal Society, A373*, 20140147.

Gopalswamy, N. (2016). History and development of coronal mass ejections as a key player in solar terrestrial relationship. *Geoscience Letters, 3*, 8

Gosling, J. T., Baker, D. N., Bame, S. J., Feldman, W. C., Zwickl, R. D., & and Smith, E. J. (1987). Bidirectional solar wind electron heat flux events. *Journal of Geophysical Research, 92*, 8519

Gosling, J. T., Skoug, R. M., McComas, D. J., & Mazur, J. E. (2004). Correlated dispersionless structure in suprathermal electrons and solar energetic ions in the solar wind. *The Astrophysical Journal, 614*, 412.

Greco, A., Servidio, S., Matthaeus, W. H., & Dmitruk, P. (2010). Intermittent structures and magnetic discontinuities on small scales in MHD simulations and solar wind. *Planetary and Space Science, 58*, 1895.

Haaland, A., Eriksson, A., Engwall, E., Lybekk, B., Nilsson, H., Pedersen, A., Svenes, K., Andre, M., Forster, M., Li, K., Johnsen, C., & Ostgaard, N. (2012). Estimating the capture and loss of cold plasma from ionospheric outflow, *Journal of Geophysical Research, 117*, A07311.

Hadid, L. Z., Sahraoui, F., & Galtier, S. (2017). Energy cascade rate in compressible fast and slow solar wind turbulence. *The Astrophysical Journal, 838*, 9.

Hartinger, M. D.; Welling, D.; Viall, N. M.; Moldwin, M. B.; Ridley, A. (2014) The effect of magnetopause motion on fast mode resonance, Journal of Geophysical Research: Space Physics, 119, 8212

Heidrich-Meisner, V., Berger, L., & Wimmer-Schweingruber, R. F. (2018). Disparity among low first ionization potential elements. *Astronomy & Asrophysics, 619*, A79

Hellinger, P., Matteini, L., Stverak, S., Travnicek, P. M., &. Marsch, E. (2011). Heating and cooling of protons in the fast solar wind between 0.3 and 1 AU: Helios revisited. *Journal of Geophysical Research, 116*, A09105.

Hesse, M., & Cassak, P. A. (2019). Magnetic Reconnection in the Space Sciences: Past, Present, and Future. Journal of Geophysical Research: Space Physics, 124. https://doi.org/10.1029/2018JA025935

Hickman, K. S., Godinez, H. C., Henney, C. J., & Arge, C. N. (2015). Data assimilation in the ADAPT photospheric flux transport model. *Solar Physics, 290*, 1105

Higginson, A. K., Antiochos, S. K., DeVore, C. R., Wyper, P. F., & Zurbuchen, T. H. (2017a). Formation of heliospheric arcs of slow solar wind. *The Astrophysical Journal Letters, 840*, L10.

Higginson, A. K.; Antiochos, S. K.; DeVore, C. R.; Wyper, P. F.; Zurbuchen, T. H. (2017b) Dynamics of Coronal Hole Boundaries, The Astrophysical Journal, 837, 113
Higginson, A. K.; Lynch, B. J., (2018) Structured Slow Solar Wind Variability: Streamer-blob Flux Ropes and Torsional Alfvén Waves, The Astrophysical Journal, 859, 6
Hiremath, K. M., & Hedge, M. (2013). Rotation rates of coronal holes and their probable anchoring depths, *The Astrophysical Journal, 763*, 137, 2013.
Hollweg, J. V., Verscharen, D., Chandran, B. D. G. (2014) Magnetohydrodynamic Slow Mode with Drifting He++: Implications for Coronal Seismology and the Solar Wind, (2014) *The Astrophysical Journal, 788*, 35.
Horbury, T. S., Forman, M. A., & Oughton, S. (2005). Spacecraft observations of solar wind turbulence: an overview. *Plasma Physics and Controlled Fusion, 47*, B703
Horbury, T. S., Matteini, L., & Stansby, D. (2018). Short, large-amplitude speed enhancements in the near-Sun fast solar wind. *Monthly Notices of the Royal Astronomical Society, 478*, 1980
Howard, R. A., et al. (2008), Sun Earth Connection Coronal and Heliospheric Investigation (SECCHI), Space Science Reviews, 136, 67
Howard, R. A., Vourlidas, A., Korendyke, C., Plunkett, S. P., et al. (2013) The solar oriber imager (SoloHI) instrument for the Solar Orbiter mission. *Proceedings of the SPIE, 8862*, 1
Howes, G. G. (2015). A dynamical model of plasma turbulence in the solar wind. *Philosophical Transactions of the Royal Society, A373*, 20140145.
Howes, G. G. (2017). A prospectus on kinetic heliophysics. Physics of Plasmas, 24, 055907.
Innes, D. E.; Bučík, R.; Guo, L. -J.; Nitta, N. (2016) Observations of solar X-ray and EUV jets and their related phenomena, Astronomische Nachrichten, Vol.337, Issue 10, p.1024
Jackson, B. V., Buffington, A., Hick, P. P., Altrock, R. C., Figueroa, S., Holladay, P. E., Johnston, J. C., Kahler, S. W., Mozer, J. B., Price, S., Radick, R. R., Sagalyn, R., Sinclair, D., Simnett, G. M., Eyles, C. J., Cooke, M. P., Tappin, S. J., Kuchar, T., Mizuno, D. Webb, D. F., Anderson, P. A., Keil, S. L., Gold, R. E., & Waltham, N. R. (2004). The Solar Mass-Ejection Imager (SMEI) mission. *Solar Physics, 225*, 177.
Kahler, S. W., Arge, C. N., & Smith, D. A. (2016). Using the WSA model to test the Parker spiral approximation for SEP event magnetic connections. *Solar Physics, 291*, 1829
Karpen, J. T.; DeVore, C. R.; Antiochos, S. K.; Pariat, E. (2017) Reconnection-Driven Coronal-Hole Jets with Gravity and Solar Wind, The Astrophysical Journal, 834, 62
Kasper, J. C., Stevens, M. L., Lazarus, A. J., Steinberg, J. T., & Ogilvie, K. W. (2007). Solar wind helium abundance as a function of speed and heliographic latitude: Variation through the solar cycle. *The Astrophysical Journal, 660*, 901.
Kasper, J. C., Stevens, M. L., Korreck, K. E., maruca, B. A., Kiefer, K. K., Schwadron, N. A., & Lepri, S. T. (2012). Evolution of the relationships between helium abundance, minor ion charge state, and solar wind speed over the solar cycle. *The Astrophysical Journal, 745*, 162.
Kasper, J. C., Bale, S. D., Belcher, J. W., Bertomier, M., et al. (2019). Alfveic velocity spikes and rotational flows in the near-Sun solar wind. *Nature, 576*, 2019
Kepko, L., Spence, H. E., & Singer, H. J. (2002). ULF waves in the solar wind as direct drivers of magnetospheric pulsations. *Geophysical Research Letters, 29,* 1197.
Kepko, L., Viall, N. M., (2019) The source, significance, and magnetospheric impact of periodic density structures within stream interaction regions, Journal of Geophysical Research, 124, 10.

Kepko, L., Viall, N. M., Antiochos, S. K., Lepri, S. T., Kasper, J. C., & Weberg, M. (2016). Implications of L1 observations for slow solar wind formation by solar reconnection. *Geophysical Research Letters, 43,* 4089.

Kessel, R. L. (2008), Solar wind excitation of Pc5 fluctuations in the magnetosphere and on the ground, Journal of Geophysical Research: Space Physics, 113, A04202

Kilpua, E. K. J., Lugaz, N., Mayx, M. L., & Temmer, M. (2019). Forecasting the structure and orientation of Earthbound coronal mass ejections. *Space Weather, 17,* 498

Kilpua, E., Koskinen, H.E.J. & Pulkkinen, T.I., (2017), Coronal mass ejections and their sheath regions in interplanetary space, *Living Rev Sol Phys, 14*, 5.

King, J. H., & Papitashvili, N. E. (2005). Solar wind spatial scales in and comparisons of hourly Wind and ACE plasma and magnetic field data. *Journal of Geophysical Research, 110,* 2104.

Klimchuk, J. A. (2012). The role of type II spicules in the upper solar atmosphere. *Journal of Geophysical Research, 117*, A12102.

Klimchuk, J. A. 2015, Phil. Trans. R. Soc. A, 373: 20140256 (http://dx.doi.org/10.1098/rsta.2014.0256)

Knetter, T., Neubauer, F. M., Horbury, T., & Balogh, A. (2004). Four-point discontinuity observations using Cluster magnetic field data: A statistical survey. *Journal of Geophysical Research, 109,* A06102.

Kocharov, L., Laitinnen, T., Usoskin, I., & Vainio, R. (2014). Transmission and emission of solar energetic particles in sem-transparent shocks. *The Astrophysical Journal Letters, 787*, L21.

Komar, C. M., Fermo, R. L., & Cassak, P. A. (2015). Comparative analysis of dayside magnetic reconnection models in global magnetosphere simulations. *Journal of Geophysical Research, 120,* 276.

Kopp, R. A., Poletto, G., Noci, G., & Bruner, M. (1985). Analysis of loop flows observed on 27 March, 1980 by the UVSP instrument during the Solar Maximum Mission. *Solar Physics, 98,* 91.

Korotova, G. I.; Sibeck, D. G. (1995) A case study of transient event motion in the magnetosphere and in the ionosphere, Journal of Geophysical Research, 100, 35.

Kraichnan, R. H. (1965) Inertial-range spectrum of hydromagnetic turbulence. *Physics of Fluids, 8,* 1385.

Krieger, A. S., Timothy, A. F., & Roelof, E. C. (1973). A coronal hole and its identification as the source of a high velocity solar wind stream. *Solar Physics, 29,* 505.

Krista, L. D., & Gallagher, P. T. (2009). Automated coronal hole detection using local intensity thresholding techniques. *Solar Physics, 256,* 87

Krista, L. D., Gallagher, P. T., & Bloomfield, D. S. (2011). Short-term evolution of coronal hole boundaries. *The Astrophysical Journal Letters, 731*, L26.

Lacombe, C., Salem, C., Mangeney, A., Hubert, D., Perche, C., Bougeret, J.-L., Kellogg, P. J., & Bosqued, J.-M. (2002). Evidence for the interplanetary electric potential? WIND observations of electrostatic fluctuations. *Annales Geophysicae, 20,* 609.

Laming, J.M. (2015) The FIP and Inverse FIP Effects in Solar and Stellar Coronae *Living Rev. Sol. Phys. 12*: 2. https://doi.org/10.1007/lrsp-2015-2

Laming, J. Martin; Vourlidas, Angelos; Korendyke, Clarence; Chua, Damien; Cranmer, Steven R.; Ko, Yuan-Kuen; Kuroda, Natsuha; Provornikova, Elena; Raymond, John C.; Raouafi, Nour-Eddine; Strachan, Leonard; Tun-Beltran, Samuel; Weberg, Micah; Wood, Brian E. (2019) Element Abundances: A New Diagnostic for the Solar Wind, The Astrophysical Journal, 879, 124

Lamy, H., Maksimovic, M., Pierrard, V., & Lemaire, J. (2003). Solar wind kinetic exospheric models with typical coronal holes exobase conditions. *AIP Conference Proceedings, 679*, 367

Landi, E., Alexander, R. L., Gruesbeck, J. R., Gilbert, J. A., Lepri, S. T., Manchester, W. B., & Zurbuchen, T. H. (2012). Carbon ionization stages as a diagnostic of the solar wind. *The Astrophysical Journal, 744*, 100.

Landi, E., Gruesbeck, J. R., Lepri, S. T., Zurbuchen, T. H., & Fisk, L. A. (2012b). Charge state evolution in the solar wind. II. Plasma charge state composition in the inner corona and accelerating fast solar wind. *The Astrophysical Journal, 761*, 48

Leamon, R. J., Smith, C. W., Ness, N. F., & Wong, H. K. (1999). Dissipation range dynamics: Kinetic Alfvén waves and the importance of β_e, *Journal of Geophysical Research, 104*, 22331.

Lemaire, J. (2012). Half a century of kinetic solar wind models. *AIP Conference Proceedings, 1216*, 8.

Lepri, S. T., Landi, E., & Zurbuchen, T. H. (2013). Solar Wind Heavy Ions over Solar Cycle 23: ACE/SWICS Measurements. *The Astrophysical Journal.* 768, 94.

Li, G., & Qin, G. (2011). A solar wind model with current sheets. *ASP Conference Series,* 444, 117.

Li, G. (2017). Particle acceleration and transport in the inner heliosphere. *Science China Earth Science, 60*, 1440.

Lie-Svendsen, O., & Leer, E. (2000). The electron velocity distribution in the high-speed solar wind: Modeling the effects of protons. *Journal of Geophysical Research, 105*, 35.

Lionello, R., Riley, P., Linker, J. A., Mikić, Z., (2005) The Effects of Differential Rotation on the Magnetic Structure of the Solar Corona: Magnetohydrodynamic Simulations, The Astrophysical Journal, 625, 463

Lionello, R.; Török, T.; Titov, V. S.; Leake, J. E.; Mikić, Z.; Linker, J. A.; Linton, M. G. (2016) The Contribution of Coronal Jets to the Solar Wind, The Astrophysical Journal Letters, 831, L2

Liou, K.; Takahashi, K.; Newell, P. T.; Yumoto, K. (2008) Polar Ultraviolet Imager observations of solar wind-driven ULF auroral pulsations, Geophysical Research Letters, Volume 35, Issue 16, CiteID L16101

Lin, Y., Duan, X, Zhao, C., & Xu, L. (2013). *Systems Science Methodological Approaches*. Sect. 7.2.2, CRC Press, Boca Raton, Florida.

Linker, J. A., Caplan, R. M., Downs, C., Lionello, R., Riley, P., Mikic, Z., Henney, C. J., Arge, C. N., Kim, T., & Pogorelov, N. (2016). An empirically driven time-dependent model of the solar wind. *Journal of Physics: Conference Series, 719*, 012012

Linker, J. A., Caplan, R. M., Downs, C., Riley, P., Mikic, Z., Lionello, R., Henney, C. J., Arge, C. N., Liu, Y., Derosa, M. L., Yeates, A., & Owens, M. J. (2017). The open flux problem. *The Astrophysical Journal, 848*, 70

Loureiro, N., & Boldyrev, S. (2017). Collisionless reconnection in magnetohydrodynamic and kinetic turbulence. *The Astrophysical Journal, 850*, 182.

Luhmann, J. C., Petrie, G., & Riley, P. (2013). Solar originsd of solar wind properties during the cycle 23 solar minimum and rising phase of cycle 24. *Journal of Advanced Research, 4,* 221.

Lynch, B. J., Edmondson, J. K., Li, Y., (2014), Interchange Reconnection Alfvén Wave Generation, Solar Physics, 289, 3043

MacNeice, P., Jian, L. K., Antiochos, S. K., Arge, C. N., Bussy-Virat, C. D., De Rosa, M. L., Jackson, B. V., Linker, J. A., Mikic, Z., Owens, M. J., Ridley, A. J., Riley, P., Savani, N., &

Sokolov, I. (2018) Assessing the quality of models of the ambient solar wind. S*pace Weather, 16*, 1644

Maksimovic, M., Zouganelis, I., Chaufray, J.-Y., Issautier, K., Scime, E. E., Littleton, J. E., Marsch, E., McComas, D. J., Salem, C., Lin, R. P., & Elliott, H. (2005). Radial evolution of the electron distribution functions in the fast solar wind between 0.3 and 1.5 AU. *Journal of Geophysical Research, 110*, A09104.

Malandraki, O. (2015). Heliospheric energetic particles and galactic cosmic ray modulation. *Journal of Physics: Conference Series, 632,* 012070.

Mandrini, C. H., Nuevo, F. A., Vásquez, A. M., Démoulin, P., van Driel-Gesztelyi, L., Baker, D., Culhane, J. L., Cristiani, G. D., Pick, M (2014), How Can Active Region Plasma Escape into the Solar Wind from Below a Closed Helmet Streamer? *Solar Physics, 289*, 11

Mangeney, A., Salem, C., Lacombe, C., Bougeret, J.-L., Perche, C., Manning, R., Kellogg, P. J., Goetz, K., Monson, S. J., & Bosqued, J.-M. (1999). WIND observations of coherent electrostatic waves in the solar wind. *Annales Geophysicae 17*, 307.

Marsch, E. (2006). Kinetic physics of the solar corona and solar wind. *Living Rev. Solar Physics 3*, 1, ttps://link.springer.com/article/10.12942/lrsp-2006-1.

Marsch, E. (2018). Solar wind and kinetic heliophysics. *Annales Geophysicae, 36*, 1607.

Marsch, E., Muhlhauser, K.-H., Rosenbauer, H., Schwenn, R., & Neubauear, F. M. (1982). Solar wind helium ions: Observations of the Helios solar probes between 0.3 and 1 AU. *Journal of Geophysical Research, 87*, 35.

Mason, E. I., Antiochos, S. K., Viall, N. M., (2019) Observations of Solar Coronal Rain in Null Point Topologies, ApJ, 874, L33

Masson, S., McCauley, P., Golub, L., Reeves, K. K., DeLuca, E. E. (2014) Dynamics of the Transition Corona, The Astrophysical Journal, 787, 145

Matsuoka, H., Takahashi, K.; Yumoto, K.; Anderson, B. J.; Sibeck, D. G. (1995) Observation and modeling of compressional Pi 3 magnetic pulsations, Journal of Geophysical Research, 100, 12103

Matteini, L., Hellinger, P., Landi, S., Travnicek, P. M., & Velli, M. (2012). Ion kinetics in the solar wind: Coupling global expansion to local microphysics. *Space Science Reviews, 172,* 373.

Matteini, L. (2016). Kinetic instabilities in the solar wind: A short review. *AIP Conference Proceedings, 1720*, 030003.

Matthaeus, W. H., & Goldstein, M. L. (1982). Measurement of the rugged invariants of magnetohydrodynamic turbulence in the solar wind. *Journal of Geophysical Research, 87*, 6011

Matthaeus, W. H, & Velli, M. (2011). Who needs turbulence? A review of turbulence effects in the heliosphere and on the fundamental process of reconnection. *Space Science Reviews, 160,* 145.

Matthaeus, W. H., Goldstein, M. L., & Montgomery, D. C., Turbulent generation of outward-traveling interplanetary Alfvénic fluctuations. (1983). *Physical Review Letters, 51*, 1484

Matthaeus, W. H., Goldstein, M. L., & Roberts, D. A. (1990). Evidence for the presence of quasi-two-dimensional nearly incompressible fluctuations in the solar wind. *Journal of Geophysical Research, 95*, 20673.

Matthaeus, W. H., Pouquet, A., Mininni, P. D., Dmitruk, P., & Breech, B. (2008). Rapid alignment of velocity and magnetic field in magnetohydrodynamic turbulence. *Physical Review Letters, 100*, 085003

McComas, D. J., Bame, S. J., Barraclough, B. L., Feldman, W. C., Funsten, H. O., Gosling, J. T., Riley, P., Skoug, R., Balogh, A., Forsyth, R., Goldstein, B. E., & Neugebauer, M. (1998). Ulysses' return to the slow solar wind. *Geophysical Research Letters, 25*, 1.

McComas, D. J., Chritian, E. R., Cohen, C. M. S., Cummings, A. C., et al. (2019). Probing the energetic particle environment near the Sun. *Nature, 576*, 223

McCracken, K. G., & Ness, N. F. (1966). The collimation of cosmic rays by the interplanetary magnetic field. *Journal of Geophysical Research, 71*, 3315.

McCraken, K. C., Rao, U. R., & Ness, N. F. (1968). Interrelationship of cosmic-ray anisotropies and the interplanetary magnetic field. *Journal of Geophysical Research, 73*, 4159.

McIntosh, S. W., De Pontieu, B., Garlsson, M., Hansteen, V., Boerner, P., & Goossens, M. (2011). Alfvén waves with sufficient energy to power the quiet solar corona and fast solar wind. *Nature, 475*, 477.

Meyer-Vernet, N., Mangeney, A., Maksimovic, M., Pantellini, F., & Issurtier, K. (2003). Some basic aspects of solar wind acceleration. *AIP Conference Proceedings, 679*, 263.

Michel, F. C. (1967). Model of solar wind structure. *Journal of Geophysics Research, 72*, 1917

Muller, D., Marsden, R. G., St. Cyr, O. C., & Gilbert, H. R. (2013). Solar Orbiter exploring the Sun-heliosphere connection. *Solar Physics, 285*, 25

Nash, A. G., Sheeley, N. R., & Wang, Y.-M. (1988). Mechanisms for the rigid rotation of coronal holes. *Solar Physics, 117*, 359, 1988.

Nemecek, Z., Durovcova, T., Safrankova, J., Nemec, F., Matteini, L., Stansvy, D. Janitzek, N., Berger, L., & Wimmer-Schweingruber, R. F. (2000). What is the solar wind frame of reference? *The Astrophysical Journal*, AAS19472R2, in press

Ness, N. F. (1996). Pioneering the swinging 1960s into the 1970s and 1980s. *Journal of Geophysical Research, 101*, 10497.

Neugebauer, M. (1985). Alignment of velocity and field changes across tangential discontinuities in the solar wind. Journal of Geophysical Research, 90, 6627.

Neugebauer, M.; Goldstein, B. E.; McComas, D. J.; Suess, S. T.; Balogh, A. (1995) Ulysses observations of microstreams in the solar wind from coronal holes, Journal of Geophysical Research,100, 23389

Neugebauer, M., Ruzmaikin, A., & McComas, D. J. (1997). Wavelet analysis of the structure of microstreams in the polar solar wind. *AIP Conference Proceedings, 385*, 41.

Neugebauer, M. (1997) Pioneers of space physics: A career in the solar wind. *Journal of Geophysical Research, 102*, 26887.

Neugebauer, M. (2012) Evidence for Polar X-Ray Jets as Sources of Microstream Peaks in the Solar Wind, The Astrophysical Journal, 750, 50

Neugebauer, M., & Giacalone, J. (2010). Progress in the study of interplanetary discontinuities. *AIP Conference Proceedings, 1216*, 194.

Neugebauer, M., & Giacalone, J. (2015). Energetic particles, tangential discontinuities, and solar flux tubes. *Journal of Geophysical Research, 120*, 8281.

Newell, P. T., & Liou, K. (2011). Solar wind driving and substorm triggering. Journal of Geophysical Research, 116, A03229.

Obridko, V. N., & Vaisberg, O. L. (2017). On the history of the solar wind discovery. *Solar System Research, 51*, 165.

Ofman, L., Provornikova, E., Abbo, L., & Giordano, S. (2015). Three-dimensional multi-fluid model of a coronal streamer belt with a tilted magnetic dipole. *Annales Geophysicae, 33*, 47

Ogilvie, K. W., & Hirshberg, J. (1974). The solar cycle variation of the solar wind helium abundance. *Journal of Geophysical Research, 79*, 4595

Oran, R., Landi, E., van der Holst, B., Lepri, S. T., Vásquez, A. M., Nuevo, F. A., Frazin, R., Manchester, W., Sokolov, I, Gombosi, T. I., (2015) A steady-state picture of solar wind acceleration and charge state composition derived from a global wave-driven MHD model, *The Astrophysical Journal, 806*, 55.

Oughton, S., Matthaeus, W. H., Wan, M. & Osman, K. T. (2015). Anisotropy in solar wind plasma turbulence. *Philosophical Transactions of the Royal Society, A373*, 20140152.

Owens, M. J., Wicks, R. T., & Horbury, T. S. (2011). Magnetic discontinuities in the near-Earth solar wind: Evidence of in-transit turbulence or remnants of coronal structure? *Solar Physics, 269*, 411.

Owens, M. J., Crooker, N U., & Lockwood, M. (2013). Solar origin of heliospheric magnetic field inverstions: Evidence for coronal loop opening with pseudostreamers. *Journal of Geophysical Resarch, 118*, 1.

Owens, M. J., Lockwood, M., Barnard, L. A., MacNeil, A. R., (2018) Generation of Inverted Heliospheric Magnetic Flux by Coronal Loop Opening and Slow Solar Wind Release, The Astrophysical Journal Letters, 868, L14

Pagel, A. C.; Crooker, N. U.; Zurbuchen, T. H.; Gosling, J. T. (2004) Correlation of solar wind entropy and oxygen ion charge state ratio, Journal of Geophysical Research: Space Physics, 109, A01113

Panasenco, Velli, M., and Panasenco, A., Large-scale Magnetic Funnels in the Solar Corona, 2019, The Astrophysical Journal, 873:25 (14pp), https://doi.org/10.3847/1538-4357/ab017c

Parker, E. N. (1958) Dynamics of the Interplanetary Gas and Magnetic Fields, Astrophysical Journal, 128, 664

Parker, E. N. (2020) Exploring the innermost solar atmosphere, Nat Astron 4, 19–20 doi:10.1038/s41550-019-0985-7

Paz Miralles, M., & Sanchez Alveida, J. (2011). *The Sun, the Solar Wind, and the Heliosphere*. Springer, Dordrecht.

Perez, J. C., & Boldyrev, S. (2010). Numerical simulations of imbalanced strong magnetohydrodynamic turbulence. *The Astrophysical Journal Letters, 710*, L63.

Peter, H. (1998). Element fractionation in the solar chromosphere driven by ionization-diffusion processes. *Astronomy & Astrophysics, 335*, 691

Peter, H., & Marsch, E. (1998). Hydrogen and helium in the solar chromosphere: a background model for fractionation. *Astronomy & Astrophysics, 335*, 1069

Pierrard, V., Lamy, H., & Lemaire, J. (2004). Exospheric distributions of minor ions in the solar wind. *Journal of Geophysical Research, 109*, A02118.

Pierrard, V., Moschou, S. P., Lazar, M., Borremans, K., & Lopez Rosson, G. (2016). Kinetic models for space plasmas: Recent progress for the soalr wind and the Earth's magnetosphere. *AIP Conference Proceedings, 1786*, 160001.

Pilleri, P., Reisenfeld, D. B., Zurbuchen, T. H., Lepri, S.T., Shearer, P., Gilbert, J. A., von Steiger, R., & Wiens, R. C. (2015). Variations in solar wind fractionation as seen by AC/SWICS and the implications for GENESIS mission results. *The Astrophysical Journal, 812*, 1

Podesta, J. J. (2010). Solar wind turbulence: Advances in observations and theory. *Proceedings of the International Astronomical Union, 6*(S274), 295.

Podesta, J. J. (2012). The need to consider ion Bernstein waves as a dissipation channel of solar wind turbulence. *Journal of Geophysical Research, 117*, A07101.

Podesta, J. J. (2015). On the resolution of the phase space density required to obtain a specified accuracy of the solar wind bulk velocity. *Journal of Geophysical Research, 120*, 3350.

Podesta, J. J., Roberts, D. A., & Goldstein, M. L. (2007). Spectral exponents of kinetic and magnetic energy spectra in solar wind turbulence. *The Astrophysical Journal, 664*, 543.

Poletto, G. (2013). Sources of solar wind over the solar activity cycle. *Journal of Advanced Research, 4*, 215.

Pontin, D. I.; Wyper, P. F. (2015), The Effect of Reconnection on the Structure of the Sun's Open-Closed Flux Boundary, The Astrophysical Journal, 805, 39

Pucci, F., Malara, F., Perri, S., Zimbardo, G., Sorrio-Valvo, L., & Valentini, F. (2016). Energetic particle transport in the presence of magnetic turbulence: influence of spectral extension and intermittency. *Monthly Notices of the Royal Astronomical Society, 459*, 3395.

Qin, G., & Li, G. (2008). Effect of flux tubes in the solar wind on the diffusion of energetic particles. *The Astrophysical Journal, 682*, L129.

Raouafi, N. E.; Patsourakos, S.; Pariat, E.; Young, P. R.; Sterling, A. C.; Savcheva, A.; Shimojo, M.; Moreno-Insertis, F.; DeVore, C. R.; Archontis, V.; Török, T.; Mason, H.; Curdt, W.; Meyer, K.; Dalmasse, K.; Matsui, Y. (2016) Solar Coronal Jets: Observations, Theory, and Modeling, Space Science Reviews, 201, 1

Randolph, J. E. (1996). NASA Solar Probe mission and system concepts. *Advances in Space Research, 17*(3), 3.

Rappazzo, A. F., Velli, M., Einaudi, G., & Dahlburg, R. B. (2005). Diamagnetic and expansion effects on the observable properties of the slow solar wind in a coronal streamer. *The Astrophysical Journal, 633*, 474

Rappazzo, A. F., Matthaeus, W. H., Ruffolo, D., Servidio, S., Velli, M., (2012) Interchange Reconnection in a Turbulent Corona, The Astrophysical Journal Letters, 758, L14

Raymond, J. C., R. Suleiman, J. L. Kohl, (1997) Elemental abundances in coronal structures, *Sol. Phys., 175*, 645.

Reale, F. (2014). Coronal loops: Observations and modeling confined plasmas. *Living Reviews of Solar Physics, 11*, 4.

Reames, D. V. (2013). The two sources of solar energetic particles. *Space Science Reviews, 175*, 53.

Reginald, N., St. Cyr, O., Davilla, J., Rastaetter, L., & Torok, T. (2018). Evaluating uncertainties in coronal electron temperature and radial speed measurements using a simulation of the Bastille Day eruption. *Solar Physics, 293*, 82

Richardson, I. G. (2004). Energetic particles and corotating interaction regions in the solar wind. *Space Science Reviews, 111*, 267.

Richardson, J. D., & Paularena, K. I. (2001). Plasma and magnetic field correlations in the solar wind. *Journal of Geophysical Research, 106*, 239.

Riley, P., Linker, J. A., & Arge, C. N. (2015). On the role played by magnetic expansion factor in the prediction of solar wind speed. *Space Weather, 13*, 154.

Roberts, D. A., Goldstein, M. L., Klein, L. W., & Matthaeus, W. H. (1987). Origin and evolution of fluctuations in the solar wind: Helios observations and Helios-Voyager comparisons. *Journal of Geophysical Research, 92*, 12023.

Rouillard, A. P.; Lavraud, B.; Sheeley, N. R.; Davies, J. A.; Burlaga, L. F.; Savani, N. P.; Jacquey, C.; Forsyth, R. J. (2010) a White Light and In Situ Comparison of a Forming Merged Interaction Region, *The Astrophysical Journal, 719*, 1385

Rouillard A. P., et al. (2010) b, Intermittent release of transients in the slow solar wind: 1. Remote sensing observations, *Journal of Geophysical Research, 115*, 4103.

Rouillard A. P., et al. (2010) c, Intermittent release of transients in the slow solar wind: 2. In situ evidence *Journal of Geophysical Research, 115*, 4104.

Rouillard, A., Viall, N. M., Pierrard, V., Vocks, C., Higginson, A., Alexandrova, O., Matteini, L., Lavraud, B., Bemporad, A., Wu, Y., Lavarra, M., Pinto, R., Sanchez-Diaz, E., (2020) The Solar Wind, book chapter accepted for publication in "The Sun and Solar Wind," ed. N. Raouafi & A. Vourlidas (AGU; Wiley)

Safrankova, J., Nemecek, Z., Cagas, P., Prech, L. Pavlu, J., Zastenker, G. N., Riazantseva, M. O., & Koloskova, I. V. (2013). Short-scale variations of the solar wind helium abundance. *The Astrophysical Journal, 778*, 25.

Salem, C., Lacombe, C., Mangeney, A., Kellogg, P. J., & Bougeret, J.-L. (2003). Weak double layers in the solar wind and their relation to the interplanetary electric field. *AIP Conference Proceedings, 679*, 513.

Salem, C., Mangeney, A., Bale, S. D., & Veltri, P. (2009). Solar wind magnetohydrodynamics turbulence: Anomalous scaling and role of intermittency. *The Astrophysical Journal, 702*, 553

Samanta et al., (2019), Generation of solar spicules and subsequent atmospheric heating, Science, 366, 890

Sanchez-Diaz, E., Rouillard, A. P., Lavraud, B., Segura, K., Tao, C., Pinto, R. Sheeley, N. R., & Plotnikov, I. (2016). The very slow solar wind: Properties, origin and variability. *Journal of Geophysical Research, 121*, doi:10.1002/2016JA022433 [L SEP].

Sanchez-Diaz, E.; Rouillard, A. P.; Davies, J. A.; Lavraud, B.; Pinto, R. F.; Kilpua, E. (2017a) The Temporal and Spatial Scales of Density Structures Released in the Slow Solar Wind During Solar Activity Maximum, The Astrophysical Journal, 851, 32

Sanchez-Diaz, E.; Rouillard, A. P.; Davies, J. A.; Lavraud, B.; Sheeley, N. R.; Pinto, R. F.; Kilpua, E.; Plotnikov, I.; Genot, V. (2017b) Observational Evidence for the Associated Formation of Blobs and Raining Inflows in the Solar Corona, The Astrophysical Journal Letters, 835, L7

Sandahl, I., Lundstedt, H., Koskinen, H., & Glassmeir, K.-H. (1996). On the need for slar wind monitoring close to the magnetosphere. *ASP Conference Series, 95*, 300.

Sarafopoulos, D. V. (1995) Long duration Pc 5 compressional pulsations inside the Earth's magnetotail lobes, Annales Geophysicae, 13, 926

Schatten, K. H. (1971). Large-scale properties of the interplanetary magnetic field. *Reviews of Geophysics and Space Physics, 9*, 773

Schekochihin, A. A., Cowley, S. C., Dorland, W., Hammett, G. W., Howes, G. G., Quataert, E., & Tatsuno, T. (2009). Astrophysical gyrokinetics: Kinetic and fluid turbulent cascades in magnetized weakly collisional plasmas. *The Astrophysical Journal Supplement Series, 182*, 310.

Schrijver, C. J., & Siscoe, G. L. (eds.) (2009). *Heliophysics: Plasma Physics of the Local Cosmos*. Cambridge University Press, Acedemic, New York.

Schrijver, C. J., & Siscoe, G. L. (eds.) (2009). *Heliophysics: Plasma Physics of the Local Cosmos*. Cambridge University Press, Acedemic, New York.

Schrijver, C. J., Title, A. M., van Ballegooijen, A. A., Hagenaar, H. J., Shine, R. A. (1997) Sustaining the Quiet Photospheric Network: The Balance of Flux Emergence, Fragmentation, Merging, and Cancellation, The Astrophysical Journal, 487, 424

Schrijver, C.J. & DeRosa, M.L., (2003) Photospheric and heliospheric magnetic fields, Sol Phys 212: 165. https://doi.org/10.1023/A:1022908504100
Schwadron, N. A.; McComas, D. J. (2003) Solar Wind Scaling Law, The Astrophysical Journal, 599, 1395
Schwartz, S. J., Paschmann, G., Sckopke, N., Bauer, T. M., Dunlop, M., Fazakerley, A. N., Thomsen, M. F. (2000). Conditions for the formation of hot flow anomalies at Earth's bow shock. *Journal of Geophysical Research, 105*, 12639.
Schwenn, R., and Marsch, E. (Eds.) (1991a). *Physics of the Inner Heliosphere 1. Large-Scale Structure*. Springer-Verlag, Berlin.
Schwenn, R., and Marsh, E. (Eds.) (1991b). *Physics of the Inner Heliosphere 2. Particles, Waves, and Turbulence.* Springer-Verlag, Berlin.
Schwenn, R., Muhlhauser, K.-H., Marsch, E., & Rosenbauer, H. (1981). Two states of the solar wind at the time of solar activity minimum II. Radial gradients of plasma parameters in fast and slow streams. in *Solar Wind Four*, MPAE-W-100-81-31, pg. 126, Max Planck Institut fur Aeronomie, Lindau, Germany.
Shi, M., Li, H., Xiao, C., & Wang, X. (2017). The parametric decay instability of Alfvén waves in turbulent plasmas and the applications in the solar wind. *The Astrophysical Journal, 842*, 63.
Sheeley, Jr., N. R. (1980). Temporal variation of loop structures in the solar atmosphere. *Solar Physics, 66*, 79.
Sheeley, N. R., Jr.; Lee, D. D. -H.; Casto, K. P.; Wang, Y. -M.; Rich, N. B. (2009) The Structure of Streamer Blobs, The Astrophysical Journal, 694, 1471
Siscoe, G. L., Davis, L., Coleman, P. J., Smith, E. J., & Jones, D. E. (1968). Power spectra and discontinuities of the interplanetary magnetic field: Mariner 4. *Journal of Geophysical Research, 73*, 61.
Smith, C. W., Tessein, J. A., Vasquez, B. J., & Skoug, R. M. (2011). Turbulence associated with corotating interaction regions at 1 AU: Inertial range cross-helicity spectra. *Journal of Geophysical Research, 116*, A10103.
Smith, C. W., Vasquez, B. J., Coburn, J. T., Forman, M. A., & Stawarz, J. E. (2018). Correlation scales of the turbulent cascade at 1 AU. *The Astrophysical Journal, 858*, 21.
Smith, R. K., & Hughes, J. P. (2010). Ionization equilibrium timescales in collisional plasmas. *The Astrophysical Journal, 718*, 583, 2010.
Stakhiv, M., Landi, E., Lepri, S. T., Oran, R., Zurbuchen, T. H. (2015) On the Origin of Mid-latitude Fast Wind: Challenging the Two-state Solar Wind Paradigm, The Astrophysical Journal, 801,100
Stansby, D., Horbury, T. S., & Matteini, L. (2018). Diagnosing solar wind origins using in situ measurements in the inner heliosphere. Monthly Notices of the Royal Astronomical Society, 482(2), 1706– 1714. https://doi.org/10.1093/mnras/sty2814
Steinberg, J. T., Lazarus, A. J., Ogilvie, K. W., Lepping, R., & Byrnes, J. (1996). Differential flow between solar wind protons and alpha particles: First WIND observations. *Geophysical Research Letters, 23*, 1183
Stverak, S., Maksimovic, M., Travnicek, P. M., Marsch, E., Fazakerley, A. N., & Scime, E. E. (2009). Radial evolution of nonthermal electron populations in the low-latitude solar wind: Helios, Cluster, and Ulysses observations. *Journal of Geophysical Research, 114*, A05104.
Subramanian, S., Madjarska, M. S., & Doyle, J. G. (2010). Coronal hole boundaries evolution at small scales II. XRT view. Can small-scale outflows at CHBs be a source of the slow wind? *Astronomy & Astrophysics, 516*, A50.

Suess, S. T., Ko, Y.-K., von Steiger, R., & Moore, R. L. (2009). Quiescent current sheets in the solar wind and origins of slow wind. *Journal of Geophysical Research, 114*, A04103.

Susino, R., Ventura, R., Spadaro, D., Vourlidas, A., & Landi, E. (2008). Physical parameters along the boundaries of a mid-latitude streamer and its adjacent regions. *Astronomy & Astrophysics, 488*, 303.

Tautz. R. C., & Shalchi A. (2011). Simulated energetic particle transport in the interplanetary space: The Palmer consensus revisited. *Journal of Geophysical Research, 118*, 642.

Telloni, D., Perri, S., Carbone, V., & Bruno, R. (2016). Selective decay and dynamic alignment in the MHD turbulence: the role of the rugged invariants. *AIP Conference Proceedings, 1720*, 040015.

Telloni, D., Carbone, V., Perri, S., Bruno, R., Lepreti, F., & Veltri, P. (2016). Relaxation processes within flux ropes in solar wind. *The Astrophysical Journal, 826*, 205

Tenerami, A., Velli, M., & DeForest, C. (2016). Inward motions in the outer solar corona between 7 and 12 Rs: Evidence for waves or magnetic reconnection jets? *The Astrophysical Journal Letters, 825*, L3

Thieme, K. M., Schwenn, R., & Marsch, E. (1989). Are structures in high-speed streams signatures of coronal fine structures? *Advances in Space Research, 9*(4), 127.

Thompson, B. et al. (2020). Solar Flares and Coronal Mass Ejections, book chapter accepted for publication in "The Sun and Solar Wind," ed. N. Raouafi & A. Vourlidas (AGU; Wiley)

Timothy, A. F., Krieger, A. S., & Vaiana, G. S. (1975). The structure and evolution of coronal holes. *Solar Physics, 42*, 135, 1975.

Titov, V. S., Mikic, Z., Linker, J. A., Lionello, R., & Antiochos, S. K. (2011). Magnetic topology of coronal hole linkages. *The Astrophysical Journal, 731*, 111.

Tong, Y., Borovsky, J. E., & Steinberg, J. T. (2016). Using ACE-Earth magnetic connection events to measure wandering length scale of interplanetary magnetic field in the solar wind. in *2016 Los Alamos Space Weather Summer School Research Reports*, pg. 55, Report LA-UR-16-29471, Los Alamos National Laboratory, Los Alamos, New Mexico.

Török, T.; Aulanier, G.; Schmieder, B.; Reeves, K. K.; Golub, L., (2009), Fan-Spine Topology Formation Through Two-Step Reconnection Driven by Twisted Flux Emergence, The Astrophysical Journal, 704, 485

Trenchi, L., Bruno, R., Telloni, D., D'Amicis, R., Marcucci, M. F., Zurbuchen, T. H., & Weberg, M. (2013). Solar energetic particle modulation associated with coherent magnetic structures. *The Astrophysical Journal, 770*, 11.

Tsuneta, S., Ichimoto, K., Katsukawa, Y., Lites, B. W., Matsuzaki, K., Nagata, S., Orozco Suarez, D., Shimizu, T., Shimojo, M., Shine, R. A., Suematsu, Y., Suzuki, T. K., Tarbell, T. D., & Title, A. M. (2008). The magnetic landscape of the Sun's polar region. *The Astrophysical Journal, 688*, 1374

Tu, C.-Y., & Marsch, E. (1995). MHD structures, waves and turbulence in the solar wind. *Space Science Reviews, 73*, 1.

Tu, C.-Y., Marsch, E., & Thieme, K. M. (1989). Basic properties of solar wind MHD turbulence near 0.3 AU analyzed by means of Elasser variables. *Journal of Geophysical Research, 94*, 11739.

Tu, C.-Y., Zhou, C., Marsch, E., Xia, L.-D., Zhao, L., Wang, J.-X., & Wilhelm, K. (2005). Solar wind origin in coronal funnels. *Science, 308*, 519.

Tu, C.-Y., Wang, X., He, J., Marsch, E., & Wang, L. (2016). Two cases of convecting structure in the slow solar wind turbulence. *AIP Conference Proceedings, 1720*, 040017.

Ugarte-Urra, I., Warren, H. P., (2012) Is Active Region Core Variability Age Dependent? The Astrophysical Journal, 761, 21

Vaivads, A., et al. (2016) Turbulence Heating ObserveR - satellite mission proposal. *Journal of Plasma Physics, 82*, 905820501.

van Driel-Gesztelyi, L., Culhane, J. L., Baker, D., Démoulin, P., Mandrini, C. H., DeRosa, M. L., Rouillard, A. P., Opitz, A., Stenborg, G., Vourlidas, A., Brooks, D. H. (2012), Magnetic Topology of Active Regions and Coronal Holes: Implications for Coronal Outflows and the Solar Wind, *Solar Physics, 281*, 1.

Velli, M. (1993) On the propagation of ideal, linear Alfven waves in radially stratified stellar atmospheres and winds. *Astronomy & Astrophysics, 270,* 304

Velli, M., & Pruneti, F. (1997). Alfvén waves in the solar corona and solar wind. *Plasma Physics and Controlled Fusion, 39*, B317.

Verdini, A., Velli, M., & Buchlin, E. (2009). Reflection driven MHD turbulence in the solar atmosphere and wind. *Earth Moon and Planets, 104*, 121.

Verscharen, D. (2019). A step closer to the Sun's secrets. *Nature, 576,* 219

Verscharen, D., Chandran, D. G., Bourouaine, S., & Hollweg, J. V. (2015). Deceleration of alpha particles in the solar wind by instabilities and the rotational force: Implications for heating, azimuthal flow, and the Parker spiral magnetic field. *The Astrophysical Journal, 806,* 157.

Viall, N. M., De Moortel, I., Downs, C., Klimchuk, J. A., Parenti, S., & Reale, F., (2020) Coronal Heating, book chapter accepted for publication in "The Sun and Solar Wind," ed. N. Raouafi & A. Vourlidas (AGU; Wiley)

Viall, N. M., Kepko, L., & Spence, H. E. (2008). Inherent length‐scales of periodic solar wind number density structures. Journal of Geophysical Research, 113, A07101. https://doi.org/10.1029/2007JA012881

Viall, N. M., L. Kepko, and H. E. Spence (2009), a, Relative occurrence rates and connection of discrete frequency oscillations in the solar wind density and dayside magnetosphere, *J. Geophys. Res., 114*, A01201, doi:10.1029/2008JA013334.

Viall, N.M., Spence, H. E., and Kasper, J., (2009), Are periodic solar wind number density structures formed in the solar corona? *Geophysical Research Letters, 36,* https://doi.org/10.1029/2009GL041191

Viall, N. M., Spence, H. E., Vourlidas, A., & Howard, R. (2010). Examining periodic solar‐wind density structures observed in the SECCHI Heliospheric imagers. Solar Physics, 267(1), 175–202. https://doi.org/10.1007/s11207‐010‐9633‐1

Viall, N. M., & Klimchuk, J. A. (2017). A Survey of Nanoflare Properties in Active Regions Observed with the Solar Dynamics Observatory. *The Astrophysical Journal, 842*, 108.

Viall, N. M., & Vourlidas, A. (2015). Periodic density structures and the origin of the slow solar wind. *The Astrophysical Journal, 807*, 176.

Villante, U.; Di Matteo, S.; Piersanti, M. (2016) On the transmission of waves at discrete frequencies from the solar wind to the magnetosphere and ground: A case study, Journal of Geophysical Research: Space Physics, 121, 380

von der Luhe, O. (2009). History of solar telescopes. *Experimental Astronomy, 25*, 197

von Steiger, R. (2008). The solar wind throughout the solar cycle. in *The Heliosphere through the Solar Activity Cycle*, A. Balagh, L. J. Lanzerotti, and S. T. Suess (Eds.). Springer Praxis, Chichester UK.

Vourlidis, A., Davis, C. J., Eyles, C. J., Crothers, S. R., Harrison, R. A., Howard, R. A., Moses, J. D., & Socker, D. G. (2007). First direct observation of the interaction between a comet and a coronal mass ejection leading to a complete plasma tail disconnection. *The Astrophysical Journal, 668*, L79

Wallace, S., Arge, C. N., Patytichis, M., Hock-Mysliwiec, & Henney, C. J. (2019). Estimating total open heliospheric magnetic flux. *Solar Physics, 294*, 19

Walsh, B. M., Bhakyapaibul, T., & Zou, Y. (2019). Quantifying the uncertainty of using solar wind measurements for geospace inputs. *Journal of Geophysical Research, 124*, 3291

Wang, C.-P., Thorne R., Liu, T. Z., Hartinger, M. D., Nagai, T., Angelopoulos, V., Wygant, J. R., Breneman, A.,Kletzing, C., Reeves, G. D., Claudepierre, S., Spence, H. E., (2017) A multispacecraft event study of Pc5 ultralow‐frequency waves in the magnetosphere and their external drivers, Journal of Geophysical Research: Space Physics Volume 122, Issue 5 https://doi.org/10.1002/2016JA023610

Wang, Y.-M., & Sheeley, Jr., N. R. (1990). Solar wind speed and coronal flux-tube expansion. *The Astrophysical Journal, 355*, 726.

Wang, Y.M., Sheeley, N.R., Walters, J.H., Brueckner, G.E., Howard, R.A., Michels, D.J., Lamy, P.L., Schwenn, R., Simnett, G.M.: 1998, Astrophys. J. 498, L165.

Webb, G. M., Zank, G. P., Kaghashvili, E. K., & le Roux, J. A. (2006). Compound and perpendicular diffusion of cosmic rays and random walk of the field lines. I. Parallel particle transport models. *The Astrophysical Journal, 651*, 211.

Weberg, M., Zurbuchen, T., Lepri, S. (2012), ACE/SWICS Observations of Heavy Ion Dropouts within the Solar Wind, *The Astrophysical Journal, 760*, 1

Weimer, D. R. & King, J. H. (2008). Improved calculations of IMF phase-front angles and propagation time delays, *Journal of Geophysical Research, 113*, A01105

Welling, D. T., Andre, M., Dandouras, I., Delcourt, D., Fazakerley, A., Fontaine, D., Foster, J., Ilie, R., Kistler, L., Lee, J. H., Liemohn, M. W., Slavin, J. A., Wang, C.-P., Wiltberger, M., & Yau, A. (2015). The Earth:Plasma sources, losses, and transport processes. *Space Science Reviews, 192*, 145.

Wicks, R. T., Horbury, T. S., Chen, C. H. K., & Schekochihin, A. A. (2010). Power and spectral index anisotropy of the entire inertial range of turbulence in the fast solar wind. *Monthly Notices of the Royal Astronomical Society, 407*, L31

Winningham, J. D., & Gurgiolo, C. (1982). DE-2 photoelectron measurements consistent with a large scale parallel electric field over the polar cap. *Geophysical Research Letters, 9*, 977.

Xu, F., & Borovsky, J. E. (2015). A new 4-plasma categorization scheme for the solar wind. *Journal of Geophysical Research, 120*, 70.

Yau, A. W., Abe, T., & Peterson, W. K. (2007). The polar wind: Recent observations. *Journal of Atmospheric and Solar-Terrestrial Physics, 69*, 1936.

Young, P. R. 2015. Dark jets in solar coronal holes. *The Astrophysical Journal 801* (2): 124 [10.1088/0004-637x/801/2/124]

Zank, G. P. (2015). Faltering steps into the galaxy: The boundary regions of the heliosphere. *Annual Reviews of Astronomy and Astrophyscs, 53*, 449.

Zastenker, G. N., Dalin, P. A., Petrukovich, A. A., Nozdrachev, M. N., Romanov, S. A., Paularena, K. I., Richardson, J. D., Lazarus, A. J., Lepping, R. P., & Szabo, A. (2000). Solar wind

structure dynamics by multipoint observations. *Physics and Chemistry of the Earth (C), 25*, 137.
Zimbardo, G. (2005). Anomalous particle diffusion and Levy random walk of magnetic field lines in three-dimensional solar wind turbulence. *Plasma Physics and Controlled Fusion, 47*, B755.
Zimbardo, G., Perri, S., Pommois, P., & Veltri, P. (2012). Anomalous particle transport in the heliosphere. *Adv. Space Res., 49*, 1633.
Zurbuchen, T. H., Hefti, S., Fisk, L. A., Gloeckler, G., & Von Steiger, R. (1999). The transition between fast and slow solar wind from composition data. *Space Science Reviews, 87*, 353.

2140